https://doi.org/10.1093/plphys/kiad200 PLANT PHYSIOLOGY 2023: 192: 1997–2014

Plant Physiology®

Research Article

The transcription factor PbrMYB24 regulates lignin and cellulose biosynthesis in stone cells of pear fruits

Yongsong Xue [1,†] Yanfei Shan,[1,†] Jia-Long Yao [2] Runze Wang,[1] Shaozhuo Xu,[1] Dongliang Liu,[1] Zhicheng Ye,[1] Jing Lin [3] Xiaogang Li,[3] Cheng Xue [4,*] and Jun Wu [1,5,*]

1 College of Horticulture, State Key Laboratory of Crop Genetics & Germplasm Enhancement and Utilization, Nanjing Agricultural University, Nanjing, Jiangsu 210095, China
2 The New Zealand Institute for Plant & Food Research Limited, Auckland 1025, New Zealand
3 Institute of Pomology, Jiangsu Key Laboratory for Horticultural Crop Genetic Improvement, Jiangsu Academy of Agricultural Sciences, Nanjing, Jiangsu 210014, China
4 State Key Laboratory of Crop Biology, College of Horticulture Science and Engineering, Shandong Agricultural University, Tai-An, Shandong 271018, China
5 Zhongshan Biological Breeding Laboratory, No.50 Zhongling Street, Nanjing, Jiangsu 210014, China

*Author for correspondence: wujun@njau.edu.cn (J.W.), xcheng@sdau.edu.cn (C.X.)
†These authors contributed equally.
The author responsible for distribution of materials integral to the findings presented in this article in accordance with the policy described in the Instructions for Authors (https://academic.oup.com/plphys/pages/General-Instructions) is Jun Wu.

Abstract

Lignified stone cell content is a key factor used to evaluate fruit quality, influencing the economic value of pear (*Pyrus pyrifolia*) fruits. However, our understanding of the regulatory networks of stone cell formation is limited due to the complex secondary metabolic pathway. In this study, we used a combination of co-expression network analysis, gene expression profiles, and transcriptome analysis in different pear cultivars with varied stone cell content to identify a hub MYB gene, *PbrMYB24*. The relative expression of *PbrMYB24* in fruit flesh was significantly correlated with the contents of stone cells, lignin, and cellulose. We then verified the function of PbrMYB24 in regulating lignin and cellulose formation via genetic transformation in homologous and heterologous systems. We constructed a high-efficiency verification system for lignin and cellulose biosynthesis genes in pear callus. PbrMYB24 transcriptionally activated multiple target genes involved in stone cell formation. On the one hand, PbrMYB24 activated the transcription of lignin and cellulose biosynthesis genes by binding to different *cis*-elements [AC-I (ACCTACC) element, AC-II (ACCAACC) element and MYB-binding sites (MBS)]. On the other hand, PbrMYB24 bound directly to the promoters of *PbrMYB169* and *NAC STONE CELL PROMOTING FACTOR* (*PbrNSC*), activating the gene expression. Moreover, both PbrMYB169 and PbrNSC activated the promoter of *PbrMYB24*, enhancing gene expression. This study improves our understanding of lignin and cellulose synthesis regulation in pear fruits through identifying a regulator and establishing a regulatory network. This knowledge will be useful for reducing the stone cell content in pears via molecular breeding.

Introduction

Pears (genus *Pyrus*; family Rosaceae) have a long cultivation history and comprise the third most economically important fruit crop in China (Wu et al. 2013). At present, cultivated pears are divided into 2 major groups; the Asian pear includes 4 species (*Pyrus bretschneideri*, *Pyrus pyrifolia*, *Pyrus ussuriensis*, and *Pyrus sinkiangensis*), and the European pear consists of only a single species, *Pyrus communis* (Bao et al. 2007; Wu et al. 2013). Asian pear fruits have a higher stone cell content, which has a negative effect on fruit quality, compared to European pears. This is especially true in traditional pear cultivars such as 'Dangshansuli'. Stone cells, known technically as sclereids, develop thick secondary cell walls (SCWs) after the cessation of cell expansion (Zhong et al. 2019). The stone

Received November 03, 2022. Accepted February 28, 2023. Advance access publication April 3, 2023

cell content is positively correlated with lignin and cellulose content (Wang et al. 2021). In addition, the average lignin content (29.73%) of pear stone cells is higher than the cellulose content (18.03%), indicating that lignin is the main component of pear stone cells (Zhang et al. 2020). Therefore, the formation and development of stone cells are closely related to the synthesis and accumulation of lignin and cellulose in pear fruits (Martín-Cabrejas et al. 2006).

The stone cell content initially increases rapidly at the early stages and then declines at later stages of pear fruit development. Usually, stone cells begin to form from 7 to 15 days after full bloom (DAFB) and accumulate rapidly from 21 to 49 DAFB (Zhao et al. 2013; Xue et al. 2019b). A previous study identified *PbrSTONE* as a gene involved in the accumulation of stone cells and lignin in *P. bretschneideri* by using genome-wide association studies (GWAS) (Zhang et al. 2021). Recently, a NAC transcription factor (TF), NAC STONE CELL PROMOTING FACTOR (PbrNSC), which was shown to promote the lignin and cellulose biosynthesis in pear fruit, was discovered using expression quantitative trait locus (eQTL) and co-expression approaches (Wang et al. 2021). In addition, PbrMYB169 was found to positively regulate lignification in stone cell development by activating the promoters of lignin biosynthesis genes (Xue et al. 2019a). In contrast, the TFs PbKNOX1 and PbBZR1 have been shown to inhibit stone cell lignification (Cheng et al. 2019; Cao et al. 2020). Although these studies help to understand the process of fruit lignification, the connection among these regulators is still not clear. Therefore, further studies are required to establish the regulatory network involved in stone cell formation.

R2R3-MYB proteins are the most widely studied group of MYB TFs, because they play diverse roles in plant secondary metabolism, including in the phenylpropanoid, benzene, and terpenoid pathways (Van Schie et al. 2006; Soler et al. 2015; Seo and Kim 2017). Moreover, they regulate pathways involved in SCW synthesis, as demonstrated in more and more studies (Liu et al. 2015; Xu et al. 2015). A group of MYB TFs in *Arabidopsis* (*Arabidopsis thaliana*), including MYB46, MYB83, MYB85, MYB63, MYB58, MYB75, MYB26, and MYB103, are involved in lignin and cellulose synthesis (Zhong et al. 2007, 2008; McCarthy et al. 2009; Zhou et al. 2009; Bhargava et al. 2010; Geng et al. 2020). Among them, AtMYB46 and AtMYB83 are considered to be the switches that regulate SCW synthesis (Ko et al. 2009). Overexpression of *AtMYB46* or *AtMYB83* promotes the abnormal accumulation of SCWs by activating genes related to SCW synthesis (Ko et al. 2009). In addition, in the double-knockout *Arabidopsis* mutant *myb46/myb83*, SCW deposition in interfascicular fibers and vessel cells was seriously affected, resulting in seedling growth arrest (McCarthy et al. 2009).

AtMYB46 can directly regulate the expression of other *MYB* genes, including *AtMYB43*, *AtMYB63*, *AtMYB58*, and *MYB85* (Zhong et al. 2008), by targeting a 7-bp sequence [ACC(A/T)A(A/C)(T/C)] known as the secondary wall MYB-responsive element (SMRE) in the promoters. Another 8-bp sequence [(T/C)ACC(A/T)A(A/C)(T/C)], the MYB46-responsive *cis*-regulatory element (M46RE), has been identified as an AtMYB46-specific binding element (Kim et al. 2012; Ko et al. 2014). *AtMYB63* and *AtMYB58* regulate lignin synthesis by binding to AC elements in the promoter of monolignol biosynthesis genes without affecting cellulose and xylan synthesis (Zhou et al. 2009). AtMYB20, AtMYB42, AtMYB43, and AtMYB85 directly activate genes related to phenylalanine and lignin biosynthesis, as well as transcriptional repressors related to flavonoid biosynthesis (Geng et al. 2020), indicating that MYB TFs regulate SCW biosynthesis.

In general, studies on lignin and cellulose biosynthesis have been mainly conducted in model plants, while research on the regulatory networks involved in stone cell formation in pear fruits is insufficient. In this study, we functionally characterized PbrMYB24 of *P. bretschneideri* and showed that it played an essential role in regulating both lignin and cellulose biosyntheses in pear fruit stone cells. Moreover, its function was coordinated with those of PbrMYB169 and PbrNSC. The results of this study would improve our understanding of the genetic regulatory network of stone cell formation and provide knowledge for reducing fruit stone cell content.

Results

PbrMYB24 gene expression is positively correlated with stone cell formation in pear fruits

In a previous study, we constructed a lignocellulose co-expression network based on the gene expression profiles of 206 pear cultivars at a single stage and of 3 cultivars at 7 different stages of fruit development (Wang et al. 2021). Eight hub genes encoding MYB TFs were identified in the network. Genome-wide identification of the MYB family in Chinese white pear was carried out, and the *PbrMYB* genes were classified and named (Li et al. 2016). In this study, the expression levels of 2 MYB genes, *PbrMYB88* and *PbrMYB24*, were correlated with stone cell contents (correlation coefficients of 0.43 and 0.42, respectively). Transcriptome analysis showed that 2 hub genes, *PbrMYB88* and *PbrMYB24*, were specifically expressed at early stages of pear fruit development (15 and 30 DAFB) (Supplemental Fig. S1). The time of gene expression was associated with the time of stone cell formation. Furthermore, *PbrMYB24* showed a higher level of expression than *PbrMYB88* (Supplemental Fig. S1), suggesting that *PbrMYB24* might be more important than *PbrMYB88* in the regulation of stone cell formation. Therefore, *PbrMYB24* was selected for further analyses.

The lignocellulose co-expression network analysis showed that *PbrMYB24* had strong connections to lignin and cellulose biosynthesis genes and 2 key TFs, PbrMYB169 and PbrNSC (Fig. 1A). To determine the relationship between the expression level of *PbrMYB24* and the contents of stone cells, lignin, and cellulose, we analyzed 20 pear varieties that

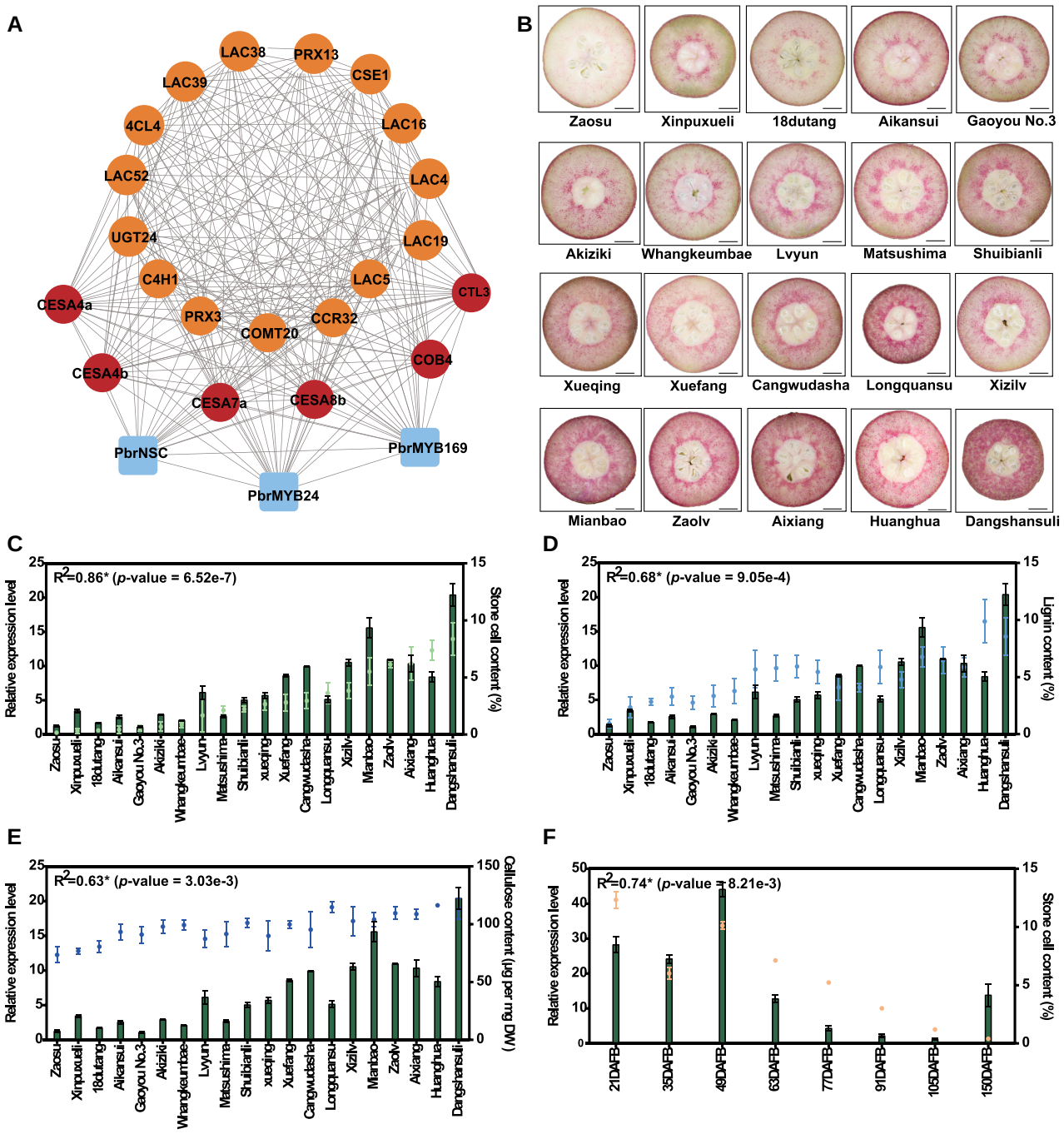

Figure 1. Co-expression network and the expression of *PbrMYB24*. **A)** The co-expression network shows that PbrMYB24 expression is highly associated with SCW biosynthesis genes and the key TFs PbrMYB169 and PbrNSC. RNA-seq data were generated using the 206 pear cultivars at 1 stage and 3 cultivars at 7 different stages of fruit development from our previous study (Wang et al. 2021). The co-expression networks comprising the credible connections were visualized using Cytoscape v3.6.0 (Shannon et al. 2003). **B)** Cross-sections of pear fruits from 20 varieties were stained with Wiesner's reagent at the key stage of stone cell formation. Scale bar = 0.5 cm. **C** to **E)** *PbrMYB24* expression levels (bar charts) are presented together with the contents (dots) of stone cell **C)**, lignin **D)**, and cellulose **E)** in the fruits of the 20 pear varieties in **B)** tested at the key stage of stone cell formation. Each value is mean ± SD ($n \geq 3$ biological replicates). Pearson's correlations were obtained using the *cor*.test. **F)** *PbrMYB24* expression levels (bar charts) are presented together with stone cell contents (dots) at 8 developmental stages DAFB of 'Dangshansuli' pear fruit. Each value is mean ± SD ($n \geq 3$ biological replicates). Pearson's correlations were obtained using the *cor*.test.

have different amounts of stone cells in their fruits, as shown by lignin staining at 35 DAFB (Fig. 1B). The expression level of *PbrMYB24* was positively correlated with stone cell content (correlation coefficient = 0.86; $P = 6.52e{-}7$), lignin content (correlation coefficient = 0.68; $P = 9.05e{-}4$), and cellulose content (correlation coefficient = 0.63; $P = 3.03e{-}3$) in the 20 pear varieties (Fig. 1, C to E).

Based on RNA-seq data from fruits at 6 development stages (15, 30, 55, 85, 115, and 130 DAFB) of 5 pear cultivars ('Dangshansuli', 'Yali', 'Hosui', 'Korla' pear, and 'Starkrimson'), *PbrMYB24* was found to be strongly expressed at the early stages (15 and 30 DAFB) of fruit development (Supplemental Fig. S1). Furthermore, reverse transcription quantitative PCR (RT-qPCR) analysis of different plant tissues from the cultivar 'Dangshansuli' showed that the expression level of *PbrMYB24* in the early stage of fruit development (21 to 49 DAFB) was substantially higher than that in the later stage of fruit development (Fig. 1F). The expression pattern of *PbrMYB24* was positively correlated with stone cell content (correlation coefficient = 0.74; $P = 8.21e{-}3$) at 8 developmental stages (21, 35, 49, 63, 77, 91, 105, and 150 DAFB) of 'Dangshansuli' pear fruit (Fig. 1F). In addition, the expression level of *PbrMYB24* in stems was significantly higher than in leaves and anthers (Supplemental Fig. S2). These results indicate that PbrMYB24 may function in regulating lignin and cellulose biosynthesis and thus stone cell formation.

PbrMYB24 is an R2R3 MYB TF related to SCW biosynthesis

To predict the function of PbrMYB24, a phylogenetic tree was constructed using the deduced amino acid sequences of stone cell biosynthesis-associated MYB TFs and a number of known R2R3 MYBs from other species that regulate the phenylpropanoid pathway (Supplemental Table S1). PbrMYB24 was found to cluster with AtMYB46, which is a known key regulator of SCW synthesis in *Arabidopsis*, indicating that PbrMYB24 is likely to play an important role in promoting SCW synthesis in pear fruits (Fig. 2A). Multiple sequence alignment analysis showed that PbrMYB24 contains

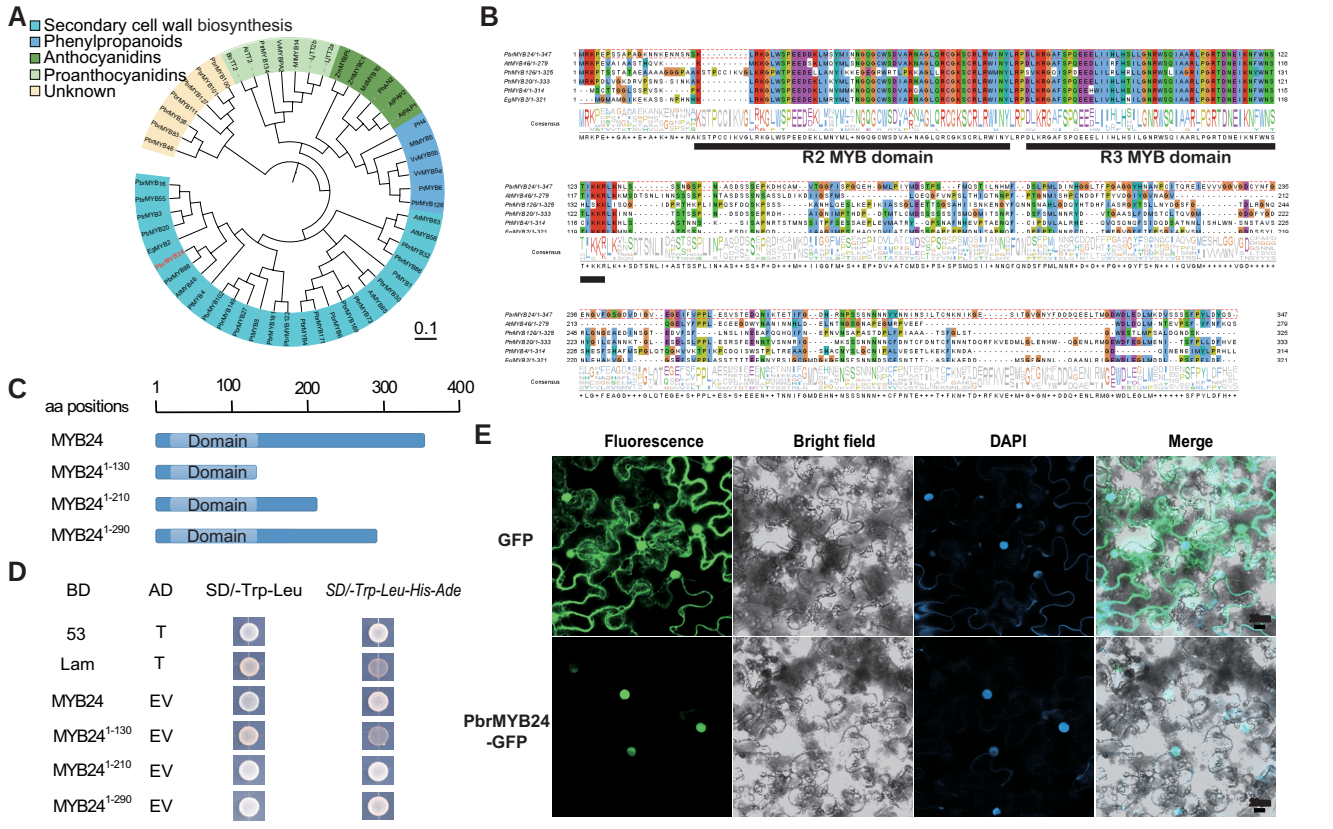

Figure 2. Amino acid sequence analysis of PbrMYB24. **A)** A phylogenetic tree showing the evolutionary relationships between stone cell biosynthesis-associated MYB TFs and a number of known R2R3 MYB TFs from other species that regulate the phenylpropanoid pathway. **B)** The alignment of the amino acid sequences of PbrMYB24, AtMYB46, PtrMYB20, PtrMYB126, PtMYB4, and EgMYB2 was generated using JALVIEW (http://www.jalview.org). At, *Arabidopsis thaliana*; Ptr, *Populus trichocarpa*; Pt, *Pinus taeda*; Eg, *Eucalyptus grandis*. **C)** Diagrams showing the structures of PbrMYB24 and the truncated proteins containing the R2R3 MYB domain. **D)** Self-activation of PbrMYB24 was demonstrated in a yeast 2-hybrid assay. SD-Trp-Leu, SD medium lacking tryptophan and leucine; SD/-Trp-Leu-His-Ade, SD medium lacking tryptophan, leucine, histidine, and adenine; BD 53-AD T interaction, positive control; BD Lam-AD T interaction, negative control; BD, DNA-binding domain; AD, activation domain. **E)** Nuclear localization of PbrMYB24 in *N. benthamiana* leaf epidermal cells was detected by transient expression of the PbrMYB24-GFP fusion protein. The nuclei were detected by DAPI staining.

typical R2- and R3-type MYB domains at its N-terminus (Fig. 2B).

To examine the subcellular localization of the PbrMYB24 protein, a PbrMYB24-GFP fusion construct was expressed in *Nicotiana benthamiana* leaves by agroinfiltration. The PbrMYB24-GFP green fluorescence signal was present specifically in the nucleus as determined by co-localization with DAPI staining, which stains DNA in the nucleus (Fig. 2E). However, the signal of GFP filled the whole cell (Fig. 2E). In addition, transactivation experiments in yeast showed that PbrMYB24 has self-activation activity, and the self-activation region is located at the N-terminal end (amino acid residues 130 to 210) of PbrMYB24 (Fig. 2, C and D). These results suggest that PbrMYB24 is a nuclear protein with transcriptional activation activity.

PbrMYB24 is involved in lignin and cellulose biosynthesis in pear fruits

To investigate the role of *PbrMYb24* in pear fruit stone cells, we generated *PbrMYB24* overexpression and silencing constructs. The constructs were separately transferred into 'Dangshansuli' pear fruit at 35 DAFB using agroinfiltration. Hand-cut sections stained with phloroglucinol-HCl showed substantially stronger lignin staining at the site injected with MYB24 overexpression construct than the site injected with the empty control vector. In contract, lignin staining was weaker at the site injected with MYB24 silencing construct than the site injected with the empty control vector (Fig. 3A). Compared with the empty vector injection sites, overexpression of *PbrMYB24* significantly increased the lignin and cellulose contents, whereas silencing of *PbrMYB24* had the opposite effect, decreasing the contents of both lignin and cellulose (Fig. 3, B and C). RT-qPCR was used to quantify the expression levels of *PbrMYB24* and lignin and cellulose biosynthesis genes at the injection sites. The results showed that regulation of *PbrMYB24* expression leads to changes in the expression levels of lignin and cellulose biosynthesis genes, especially *Pbr4CL1*, *Pbr4CL4*, *PbrCSE1*, *PbrCCOAMT6*, *PbrCCOAMT1*, *PbrLAC4*, *PbrSTONE*, and *PbrCSEA8a*, and the TF gene *PbrMYB169* (Figs. 3, D and E, and S3). These results suggest that changes in the relative expression of *PbrMYB24* regulate lignin and cellulose formation in pear fruit stone cells.

Overexpression of *PbrMYB24* promotes lignin and cellulose accumulation in pear fruit callus

To further confirm the role of *PbrMYB24* in lignin accumulation in pear fruits, the empty vector and *PbrMYB24*

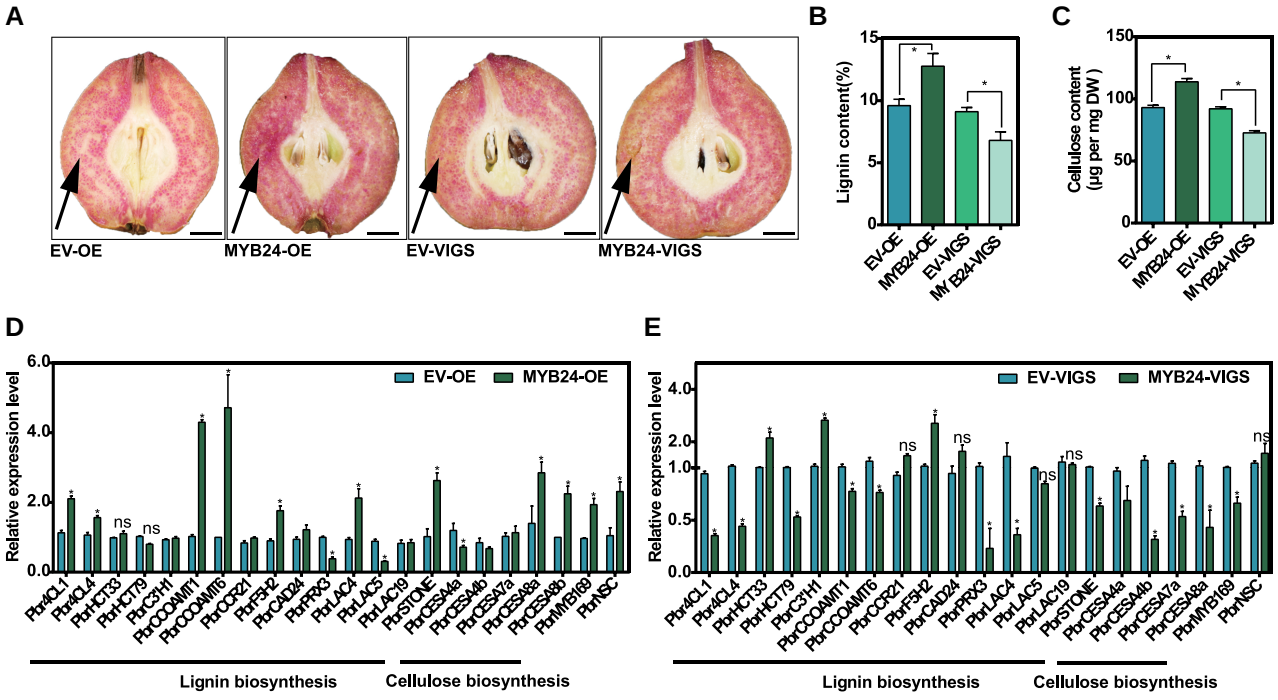

Figure 3. PbrMYB24 positively regulates lignin and cellulose biosynthesis in stone cells of pear fruits. **A)** Sections of fruit flesh transiently expressing *PbrMYB24* overexpression and silencing constructs were stained with Wiesner's reagent. EV, empty vector; OE, overexpression; VIGS, virus-induced gene silencing. Scale bar = 0.5 cm. **B, C)** Lignin **B)** and cellulose **C)** contents in pear flesh tissue around the infiltration sites were determined using the acetyl bromide and anthrone–sulfuric acid methods, respectively. Each value is mean ± SD ($n \geq 9$ biological replicates). *P*-values were tested using Student's *t* test (*$P < 0.05$). **D, E)** RT-qPCR was used to analyze the expression level of SCW biosynthesis genes and *PbrMYB169* in the pear flesh tissue around the infiltration sites. Each value is mean ± SD ($n = 3$ biological replicates). *P*-values were tested using Student's *t* test (*$P < 0.05$; ns, not significant).

overexpression construct were stably transformed into pear callus. Seven transgenic pear calli were identified, of which 3 lines (OE-2, OE-4, and OE-6) showed high levels of *PbrMYB24* expression as determined by RT-qPCR (Fig. 4A). The callus growing on MS medium supplemented with 2,4-dichlorophenoxyacetic acid (2,4-D) and 6-benzylaminopurine (6-BA) shown no staining with phloroglucinol-HCl and remained white or light yellow in color (Supplemental Fig. S4A). This indicated that there is almost no lignin biosynthesis in pear callus tissue growing on this medium. To solve this problem, we established a lignin induction system for pear callus by supplementing the medium with epibrassinolide (EBR) but without 2,4-D or 6-BA (Supplemental Fig. S4). Obvious lignin staining was observed on the medium without 2,4-D or 6-BA but with different levels (0 to 400 μM) of EBR. The lignin content tended to be stable around 20 d after treatment with EBR (Supplemental Fig. S4, A to D).

The transgenic pear calli were transferred to lignin induction medium supplemented with 10 μM EBR for 20 d and then stained with phloroglucinol-HCl. The results showed that the *PbrMYB24*-OE (overexpression) callus displayed an obvious red color, whereas the callus transformed with the empty vector stained very faintly (Fig. 4, D and E). At the same time, calcofluor white staining of cellulose gave a stronger fluorescence signal in the *PbrMYB24*-OE callus (Fig. 4, F and G). Lignin and cellulose contents were significantly increased in the *PbrMYB24*-OE callus comparing with the empty vector callus (Fig. 4, B and C). Furthermore, RT-qPCR showed that the expression levels of lignin and cellulose biosynthesis genes (*Pbr4CL1*, *PbrC3′H1*, *PbrCSE1*, *PbrHCT79*, *PbrCCR21*, *PbrCCOMT23*, *PbrCAD24*, *PbrLAC4*, *PbrLAC19*, *PbrSTONE*, *PbrCESA8b*, *PbrCESA4b*, *PbrCESA7a*, and *PbrCESA4b*) as well as 2 genes encoding TFs (*PbrMYB169* and *PbrNSC*) were significantly increased in the *PbrMYB24*-OE callus compared with the empty vector control callus (Fig. 4H). These results suggest that overexpression of *PbrMYb24* promotes lignin and cellulose accumulation in pear callus.

Overexpression of *PbrMYB24* enhances SCW biosynthesis in transgenic *Arabidopsis* plants

In order to further verify the function of *PbrMYB24*, *Agrobacterium tumefaciens* carrying the *PbrMYB24* overexpression construct was used to transform *A. thaliana* Col-0. Twelve hygromycin-resistant T_1-generation transgenic plants were identified on MS medium containing hygromycin, and 3 plants (OE-6, OE-7, and OE-10) were found to have high expression levels of *PbrMYB24* as determined by RT-qPCR (Supplemental Fig. S5A). The homozygous T_3-generation plants derived from the 3 lines were used in experiments to examine the physiological and biochemical indexes.

In the T_3-generation homozygous plants, we analyzed multiple phenotypes and the lignin content of wild-type (WT) and *PbrMYB24*-OE plants. Root lengths, rosette leaves, and primary inflorescence stem heights of the T_3 homozygous plants were similar to those of the WT control plants at 1, 2, and 6 wk of age (Supplemental Fig. S5, B to G). Total lignin and cellulose contents were significantly higher in the transgenic plants compared to WT (Fig. 5, A and B). Furthermore, RT-qPCR revealed that the expression level of *AtMYB46* regulated the downstream expression of MYB TF genes, including AtMYB85 and AtMYB63. The expression of SCW biosynthesis genes was also significantly increased in the transgenic plants compared with WT (Fig. 5C).

There was no difference in the morphology of interfascicular fiber and vessel cells between the WT and transgenic *Arabidopsis* lines as shown by toluidine blue O staining (Fig. 5, D and E), but the xylem tissue of the transgenic lines showed stronger spontaneous lignin fluorescence (Fig. 5, F and G). Furthermore, safranin O–fast green staining of lignin was stronger in the interfascicular fiber and xylem, and calcofluor white staining of cellulose gave a stronger fluorescence signal in epidermal cells in the *PbrMYB24*-OE plants, while only weak staining was observed in WT plants (Fig. 5, H to K). The SCWs of the interfascicular fiber and vessel cells were observed by transmission electron microscopy (TEM). Compared with the WT, the SCWs of the interfascicular fiber and vessel cells in the *PbrMYB24*-OE lines showed significant thickening (Fig. 5, L to Q). These results indicated that *PbrMYB24* expression facilitates lignin and cellulose accumulation and SCW thickening in the inflorescence stem of transgenic *Arabidopsis* plants.

PbrMYB24 binds to the AC elements and MBS in the promoters of SCW biosynthesis genes

In order to determine the regulatory relationship between PbrMYB24 and genes involved in SCW biosynthesis, we cloned the promoter regions of the structural genes into the pGreenII 0800-LUC vector (Supplemental Fig. S6). A dual-luciferase reporter assay indicated that PbrMYB24 could activate the promoters of 9 genes, including *Pbr4CL1*, *PbrCCR21*, *PbrCCR23*, *PbrCCOAMT1*, *PbrLAC4*, *PbrLAC19*, *PbrSTONE*, *PbrCESA8b*, and *PbrCESA8a* (Fig. 6B). Previous studies have shown that MYB proteins bind to various *cis*-elements, such as AC elements, MBSs, SMRE, and M46RE, to regulate SCW biosynthesis in model plants (Ithal and Reddy 2004; Rogers and Campbell 2004; Rahantamalala et al. 2010; Kim et al. 2012; Zhong and Ye 2012; Smita et al. 2015). After analyzing the promoters of pear lignin and cellulose biosynthesis genes using the PlantCARE database (2023), we identified at least 1 AC element or MBS in each promoter, except for the promoter of *PbrSTONE* and *PbrCESA4a* (Fig. 6A and Supplemental Table S2). However, no SMRE or M46RE was identified in any promoter.

To further verify that PbrMYB24 activates transcription from the promoters through the AC or MBS elements, dual-luciferase reporter assays were performed with mutated promoters of *Pbr4CL1*, *PbrCCOAMT1*, *PbrLAC4*, *PbrLAC19*, and *PbrCESA8b*, in which the MBS or AC elements were deleted. The results showed that deleting the AC elements from the

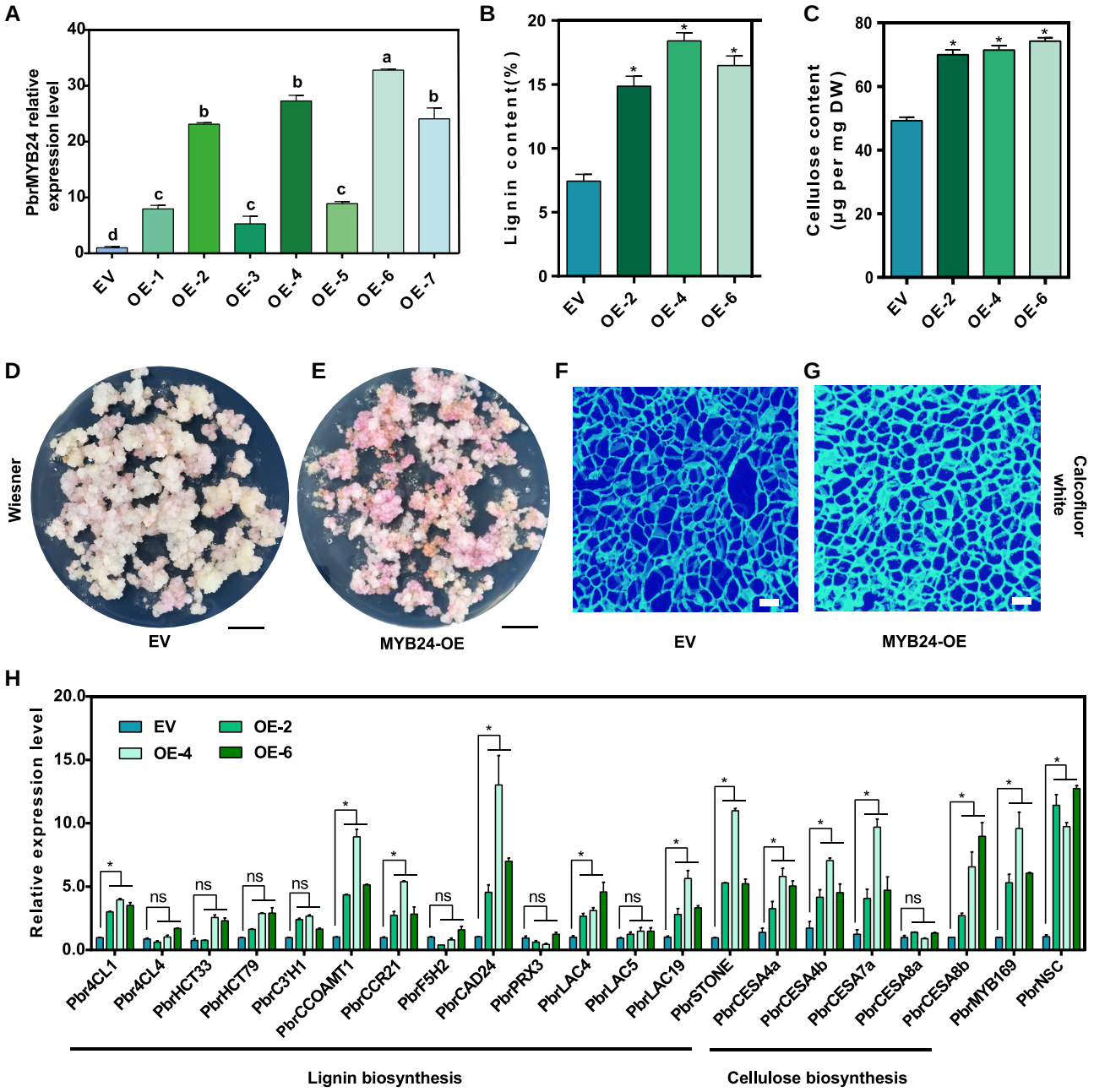

Figure 4. Overexpression of PbrMYB24 promoted lignin and cellulose accumulation in pear callus. **A)** RT-qPCR was used to analyze *PbrMYB24* expression in transgenic pear callus lines generated using either an empty vector or a vector for overexpressing *PbrMYB24* (lines OE-1 to OE-7). Each value is mean ± SD ($n = 3$ biological replicates). Groups indicated by different letters were significantly different ($P < 0.05$, 1-way ANOVA, Tukey's HSD post hoc test). **B, C)** Lignin **B)** and cellulose **C)** contents in the transgenic pear callus were determined using the acetyl bromide and anthrone–sulfuric acid methods, respectively. EV, empty vector; OE, overexpression. Each value is mean ± SD ($n \geq 9$ biological replicates). The *P*-values were tested using Student's *t* test (*$P < 0.05$). **D, E)** The transgenic pear calli were stained with Wiesner's reagent. Scale bar = 1 cm. **F, G)** Fluorescent micrographs of thin sections of transgenic pear callus that had been stained with calcofluor white. Scale bars = 50 μm. **H)** RT-qPCR was used to analyze the expression levels of SCW synthesis-related genes in the transgenic pear callus. *P*-values were tested using Student's *t* test (*$P < 0.05$; ns, not significant).

Pbr4CL1, *PbrCCOAMT1*, and *PbrLAC19* promoters prevented their activation by PbrMYB24; however, PbrMYB24 still was able to activate the promoters of *PbrLAC4* and *PbrLAC19* without an MBS (Fig. 6C). In addition, PbrMYB24 can weakly activate the promoter of *PbrCESA8b* lacking MBS2, but cannot activate the promoter of *PbrCESA8b* lacking MSB1 (Fig. 6C). These results showed that PbrMYB24 recognized AC elements in the promoters of lignin biosynthesis genes and the MBSs in the promoters of cellulose biosynthesis genes to activate their transcription.

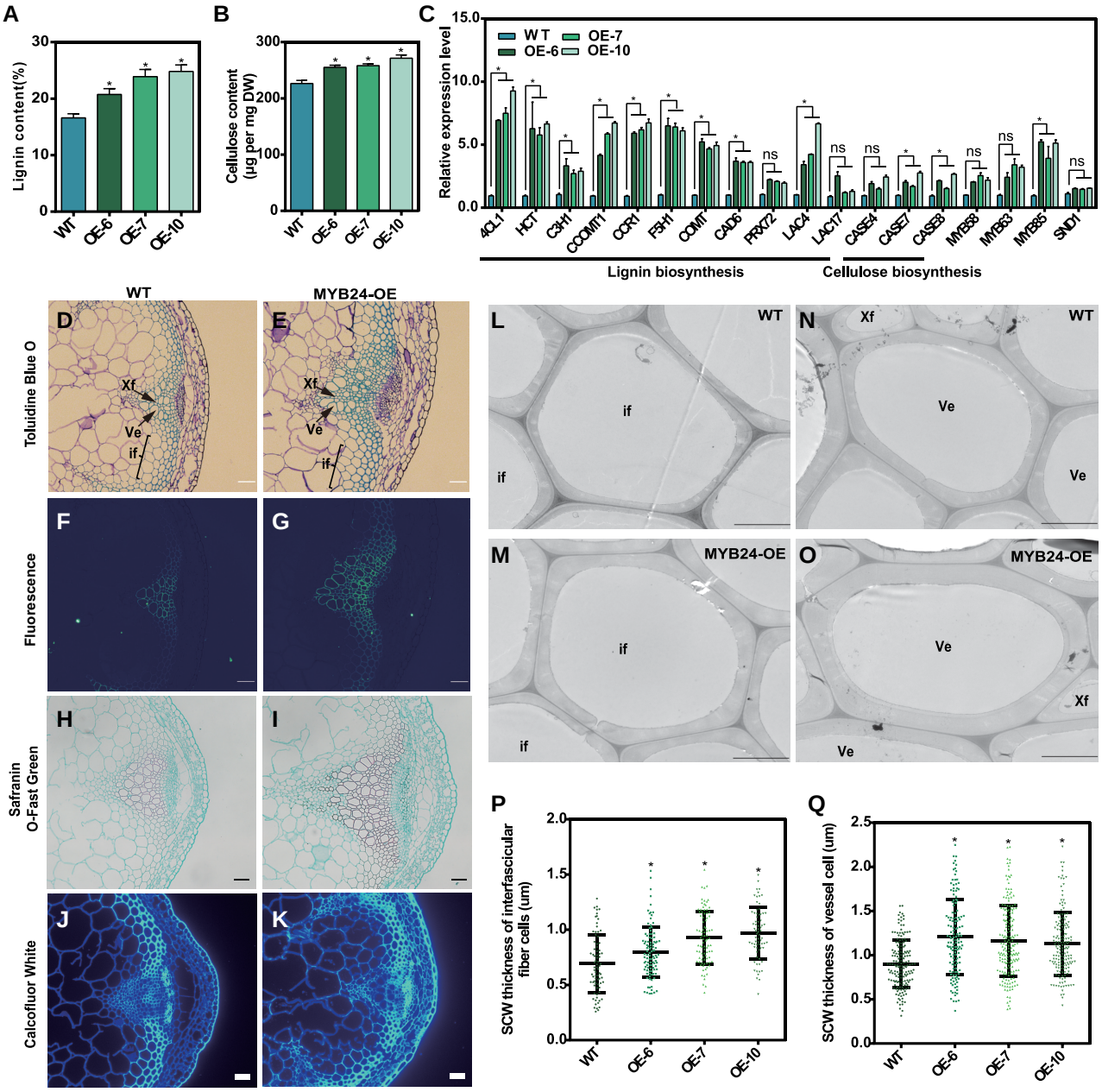

Figure 5. Functional validation of *PbrMYB24* in transgenic *Arabidopsis* plants. **A, B)** The acetyl bromide and anthrone–sulfuric acid methods were used to determine the lignin **A)** and cellulose **B)** contents of *Arabidopsis* inflorescence stems in 8-wk-old plants, respectively. OE, overexpression. Each value is mean ± SD ($n \geq 9$ biological replicates). *P*-values were tested using Student's *t* test (*$P < 0.05$). **C)** RT-qPCR was used to analyze expression levels of SCW synthesis-related genes in WT and *PbrMYB24*-OE *Arabidopsis* plants. Each value is mean ± SD ($n = 3$ biological replicates). *P*-values were tested using Student's *t* test (*$P < 0.05$; ns, not significant). **D, E)** Cross-sections of inflorescence stems were stained with toluidine blue O. Scale bars = 50 μm. Ve, vessel; Xf, xylary fiber; if, interfascicular fiber cell. **F, G)** Lignin autofluorescence in the cross-sections shown in **D, E)** was detected under UV light. Scale bars = 50 μm. **H** to **K)** Cross-sections of inflorescence stems were stained with safranin O–fast green **H, I)** or calcofluor white **J, K)**. Scale bars = 50 μm. **L** to **O)** Transmission electron micrographs of cross-sections of inflorescence stems showing interfascicular fiber cells (if) **L, M)** and vessel cells (V) **N, O)**. The image in **N)** is from the same WT *Arabidopsis* sample as that in **L)**. Bar = 5 μm. **P, Q)** The thickness of the SCWs of interfascicular fiber cells **P)** and vessel cells **Q)** were analyzed based on images similar to those shown in **L** to **O)**. The *P*-values were tested using Student's *t* test (*$P < 0.05$).

To determine whether PbrMYB24 can bind directly to the promoters of the lignin and cellulose biosynthesis genes, 1-hybrid analyses were used to examine the interaction between PbrMYB24 and the gene promoters. First, we selected promoters that are strongly activated (*Pbr4CL1*, *PbrCCOAMT1*, *PbrLAC4*, *PbrCESA8b*, and *PbrCESA8a*) and 4 mutated promoters (*Pbr4CL1-AC-D*, *PbrCCOAMT1-AC-D*, *PbrCESA8b-MBS1-D*, and *PbrCESA8b-MBS2-D*) to construct

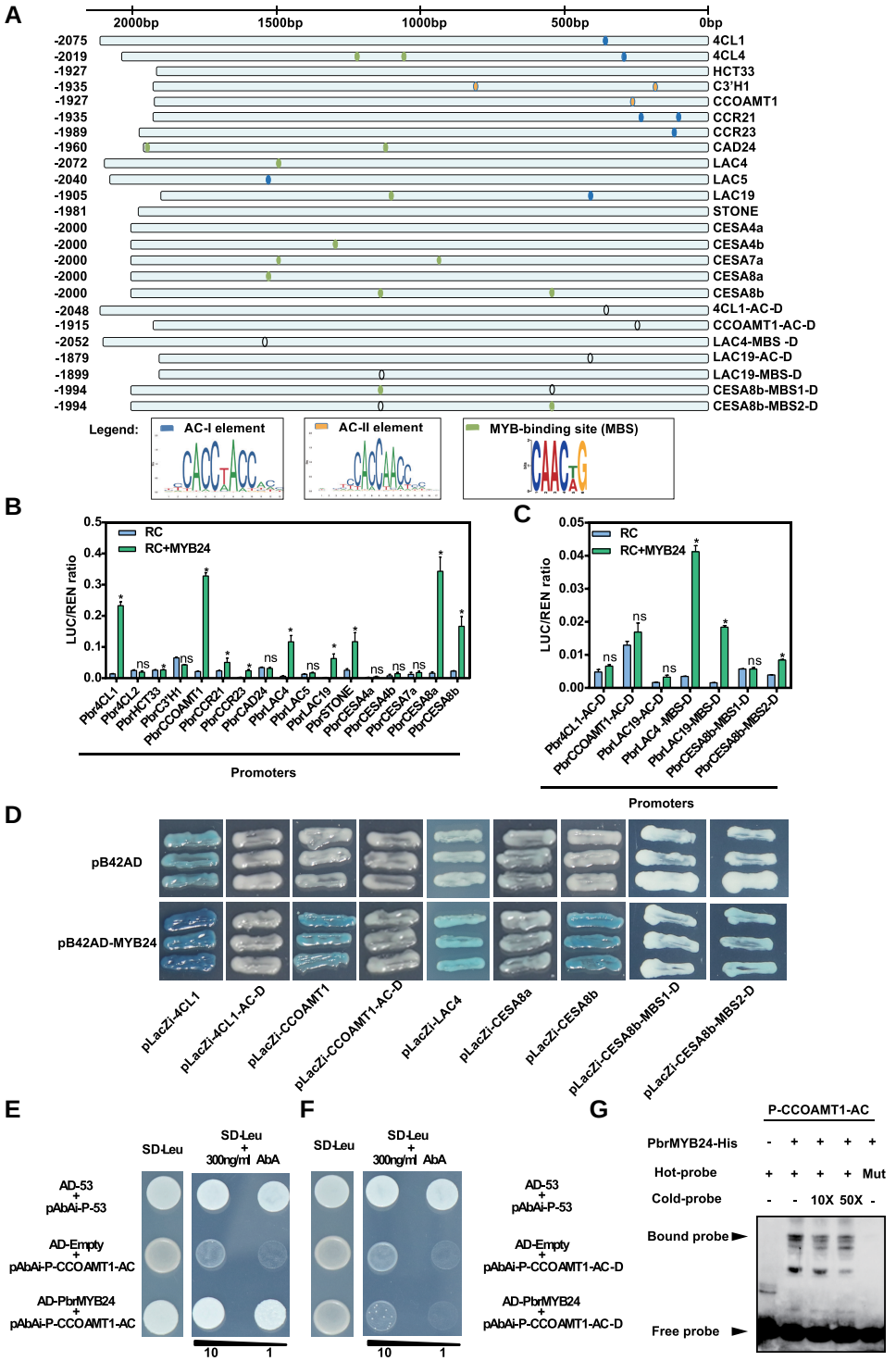

Figure 6. PbrMYB24 binds to and activates the promoters of SCW biosynthesis genes in pear. **A)** The positions of AC elements and MBS were identified in the promoter sequences of pear SCW biosynthesis genes. **B)** PbrMYB24 significantly enhanced the promoter activity of 10 lignin and cellulose biosynthesis genes as shown by dual-luciferase reporter assays in *N. benthamiana* leaf epidermal cells. *N. benthamiana* leaves were transfected with the reporter gene construct (RC) alone or co-transfected with the PbrMYB24 overexpression construct (RC + MYB24). Each value is mean ± SD ($n = 3$ biological replicates). *P*-values were tested using Student's *t* test (*$P < 0.05$; ns, not significant). **C)** PbrMYB24 was tested on mutated promoters without AC elements or MBS. Each value is mean ± SD ($n = 3$ biological replicates). *P*-values were tested using Student's *t* test (*$P < 0.05$; ns, not significant). **D)** Y1H assays showed the interaction between PbrMYB24 and the promoters of lignin and cellulose biosynthesis genes. **E, F)** PbrMYB24 binds directly to AC elements in the *PbrCCOAMT1* promoter in a Y1H assay. ABA, aureobasidin A; SD-Leu, SD medium lacking leucine. **G)** PbrMYB24 binds directly to the promoter AC elements in an EMSA. "Hot-probe" and "cold-probe" indicate the biotin-labeled and unlabeled DNA fragments, respectively.

the reporters. The yeast 1-hybrid (Y1H) system using pLacZi showed that the yeast colonies co-transformed with PbrMYB24, and the *Pbr4CL1*, *PbrCCOAMT1*, *PbrLAC4*, *PbrCESA8b*, or *PbrCESA8b-MBS2-D* promoters were blue, while the colonies co-transformed with pB42AD and the promoters were white or pale blue (Fig. 6D). In addition, the yeast colonies co-transformed with PbrMYB24 and *CESA8a* or the other 3 mutant promoters were always white (Fig. 6D). These results showed that PbrMYB24 bound directly to the AC elements present in the *Pbr4CL1* and *PbrCCOAMT1* promoters and the MBS in the *PbrCESA8b* promoter.

Second, the 300-bp promoter sequences from *Pbr4CL1* and *PbrCCOAMT1* that contain the AC elements with high activation effect were inserted into the pABAi vector. The self-activation activity of the promoters was screened using aureobasidin A (ABA). We found that 200 ng/mL ABA could inhibit the growth of yeast cells carrying pABAi-CCOAMT1-AC, but not cells carrying pABAi-4CL1-AC (Supplemental Fig. S7). The Y1H system using pAbAi showed that yeast cells co-transformed with the PbrMYB24-effector and *PbrCCOAMT1-AC*-reporter grew on SD/-Leu medium (with 0 and 300× ABA), while the yeast cells co-transformed with the PbrMYB24-effector and *PbrCCOAMT1-AC-D*-reporter did not grow normally on SD/-Leu medium (with 300× ABA), demonstrating that PbrMYB24 could bind directly to the AC elements (Fig. 6, E and F).

Finally, PbrMYB24-His fusion protein was produced by using a prokaryotic expression system (Supplemental Fig. S8) and used to verify these interactions in an electrophoretic mobility shift assay (EMSA). A DNA fragment from *PbrCCOAMT1* promoter containing the AC elements was used as the probe. When the recombinant PbrMYB24-His fusion protein was incubated with biotin-labeled probe, clear DNA–protein bands with reduced mobility were observed (Fig. 6G). The signal of the bound probe band gradually decreased as the concentration of unlabeled competitive probes was increased. All of these results indicated that PbrMYB24 specifically bound to the AC elements and MBS present in the promoters of the lignin and cellulose biosynthesis genes to promote gene expression and lead to SCW biosynthesis.

A transcriptional regulatory network consisting of PbrMYB24, PbrMYB169, and PbrNSC

In order to reveal the activation and interactions between PbrMYB24, PbrMYB169, and PbrNSC, we performed dual-luciferase reporter assays and firefly luciferase complementation imaging (LCI) in *N. benthamiana*. No LUC luminescence signal was detected in the leaves of *N. benthamiana* co-infiltrated with MYB24-cLUC and MYB169-nLUC or NSC-nLUC (Supplemental Figs. S9 and S10). This result suggests that PbrMYB24 protein was unable to bind to PbrMYB169 or PbrNSC protein. We next investigated the mutual activation among PbrMYB24, PbrMYB169, and PbrNSC to their gene promoters. Interestingly, dual-luciferase reporter assays showed that PbrMYB24 activated the full-length (2,000 bp) promoter of *PbrMYB169* and *PbrNSC* (Fig. 7, A to C) but did not activate *PbrMYB24* promoter (Fig. 7D). Furthermore, *PbrMYB24* promoter was activated by PbrMYB169 and PbrNSC (Fig. 7D). In order to identify the possible promoter binding region, 6 truncated promoters of the *PbrNSC* (−500 to 0, −1,000 to 0, and −1,500 to 0) and *PbrMYB169* (−500 to 0, −1,000 to 0, and −1,500 to 0) (Fig. 7A) were tested in dual-luciferase reporter assays. PbrMYB24 activated all but 1 truncated promoter, *PbrMYB169* promoter (−500 to 0) (Fig. 7, B and C). These results showed that PbrMYB24 recognized 2 promoter regions of *PbrNSC* (−500 to 0) and *PbrMYB169* (−1,000 to −500). As these regions do not contain any MBS, AC element, SMRE, or M46RE (Fig. 7A), PbrMYB24 might bind to some unknown elements.

To further investigate whether PbrMYB24, PbrMYB169, and PbrNSC can bind directly to their own gene promoter, the promoter regions (2 kb) upstream of *PbrMYB24*, *PbrMYB169*, and *PbrNSC* were separately cloned into the pLacZi vector to construct the reporters. The Y1H system confirmed that PbrMYB24 bound directly to the promoters of *PbrMYB169*, *PbrNSC*, and *PbrNSC-MBS-D*, but not to *PbrMYB24* promoter (Fig. 7E). Furthermore, PbrNSC bound weakly to the promoter of *PbrMYB24*, but PbrMYB169 did not bind to the *PbrMYB24* promoter (Fig. 7F). Based on these results, we deduce that PbrMYB24, PbrMYB169, and PbrNSC function in a coordinated manner to regulate lignin and cellulose biosynthesis in the formation of pear stone cells.

Discussion

PbrMYB24 is an activator for both lignin and cellulose biosyntheses in pear fruit

Previous studies have shown that lignin and cellulose synthesis is regulated by a complex transcription regulation, which contains a number of MYB TFs (Taylor-Teeples et al. 2015). Based on their regulatory effects, these MYB TFs could be future subdivided into different subgroups. For example, AtMYB85, AtMYB63, and AtMYB58 positively regulate the biosynthesis of lignin, while AtMYB4, AtMYB7, and AtMYB32 repress the program during xylem differentiation of *Arabidopsis* (Jin et al. 2000; Preston et al. 2004; Zhong et al. 2008; Geng et al. 2020). However, AtMYB46, AtMYB83, and AtMYB103 not only involve in the biosynthesis of lignin but also regulate cellulose synthesis (Zhong et al. 2008; Ko et al. 2009; Öhman et al. 2013). In pear fruits, 20 MYB TFs have been predicted to be involved in stone cell formation by genome-wide phylogenetic analyses (Cao et al. 2016). Among them, only PbrMYB169 was confirmed to specifically regulate lignin biosynthesis in stone cell (Xue et al. 2019a). At present, there are no reports on the regulation of cellulose biosynthesis in pear by MYB TFs. In this study, based on a combination of co-expression network analysis, gene expression profiles, and transcriptomic analysis in a diverse group of pear accessions, we identified a hub MYB TF,

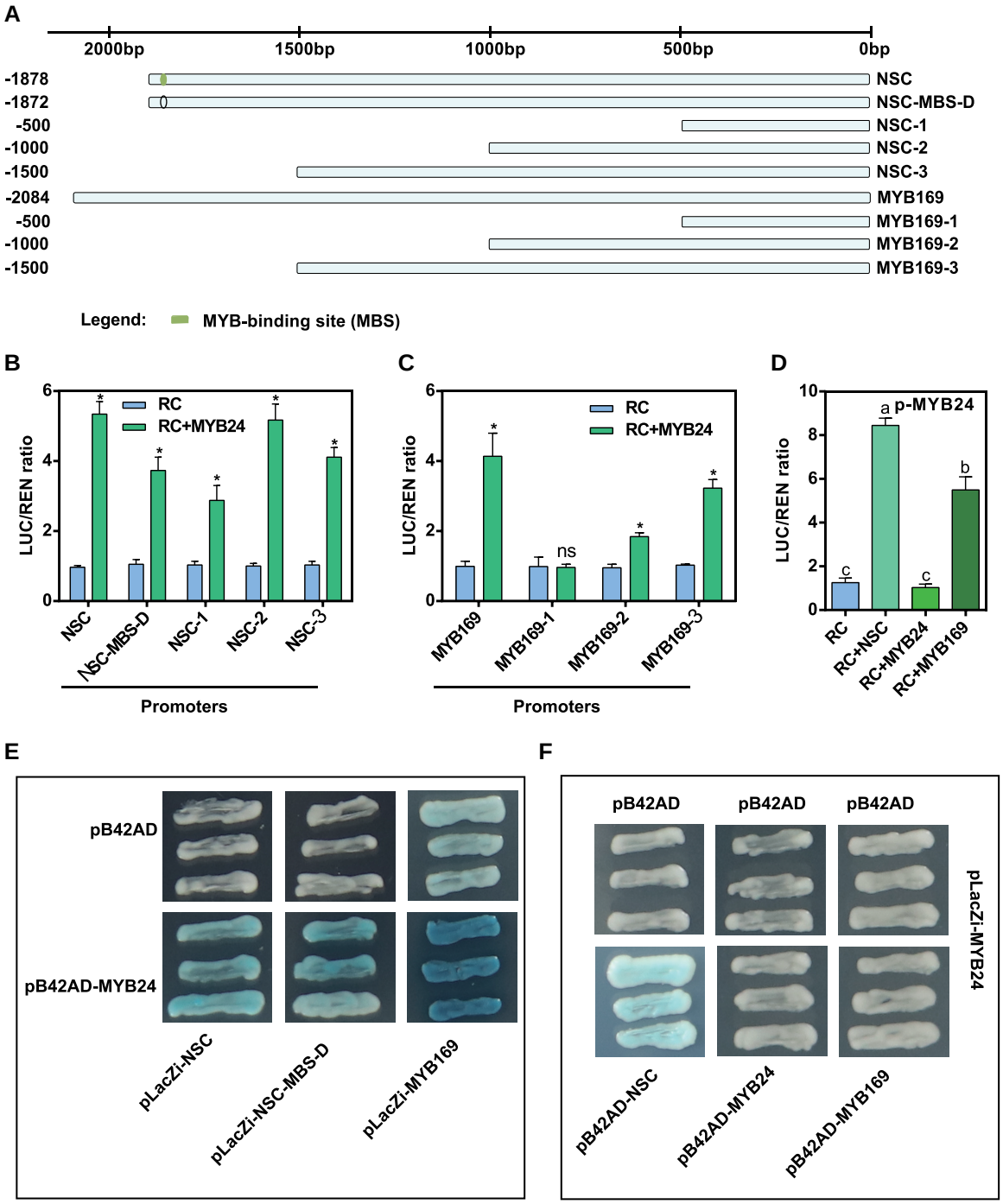

Figure 7. Dual-luciferase and Y1H assays validate the direct regulation between PbrMYB24, PbrMYB169, and PbrNSC. **A)** The diagrams show truncated promoters of *PbrNSC* and *PbrMYB169*. **B, C)** PbrMYB24 activated the *PbrMYB169* and *PbrNSC* promoters. Each value is mean ± SD ($n = 3$ biological replicates). Statistical analysis was performed using Student's *t* test (*$P < 0.05$; ns, not significant). **D)** PbrNSC and PbrMYB169 increased transcription from the *PbrMYB24* promoter. Each value is mean ± SD ($n = 3$ biological replicates). Groups indicated by different letters were significantly different ($P < 0.05$, 1-way ANOVA, Tukey's HSD post hoc test). **E, F)** Y1H assays show the interactions between PbrMYB24, PbrMYB169, and PbrNSC and their gene promoters. PbrMYB24 binds to the *PbrMYB169*, *PbrNSC*, and *PbrNSC-MBS-D* promoters, but not to its own gene promoter. PbrMYB169 cannot bind to the *PbrMYB24* promoter. PbrNSC binds weakly to the *PbrMYB24* promoter. The empty pB42AD and the *PbrMYB24*, *PbrMYB169*, and *PbrNSC* promoters cloned into pLaczi were used as the negative controls.

designated *PbrMYB24* that is positively correlated with stone cell, lignin, and cellulose. Furthermore, *PbrMYB24* was found to simultaneously promote both lignin and cellulose biosyntheses in pear flesh and callus tissue and also in the inflorescence stem of *Arabidopsis* plants, which is different from *PbrMYB169* only regulating lignin biosynthesis.

Collectively, the results of our study provide a high-quality gene resource for reducing lignin and cellulose biosynthesis in stone cells of pear fruits.

PbrMYB24 binds to different *cis*-acting elements to separately regulate the lignin and cellulose biosynthesis in stone cell of pear

Studying the combination of TFs and *cis*-elements can increase our understanding of transcriptional regulation mechanism. Previous studies have shown that MYB proteins bind to various *cis*-elements, such as AC elements, MBSs, SMRE, M46RE, and MYBCORE, to regulate different secondary metabolic pathways in plants (Ithal and Reddy 2004; Rogers and Campbell 2004; Rahantamalala et al. 2010; Kim et al. 2012; Zhong and Ye 2012; Smita et al. 2015). Although the interactions between MYB proteins and DNA motifs have been well studied in model plant, the *cis*-elements recognized by MYB TFs in the process of stone cell formation are still not well known.

In this study, dual-luciferase reporter assay and Y1H assay showed that PbrMYB24 directly activates the promoters of lignin biosynthesis genes (*Pbr4CL1*, *PbrCCOAOMT1*, and *PbrLAC4*) and cellulose biosynthesis gene *PbrCESA8b*. Further, promoter truncation test showed that PbrMYB24 directly binds to the AC elements in the promoters of *Pbr4CL1* and *PbrCCOAOMT1* and binds to MBS in the promoter of *PbrCESA8b*. These results indicate that PbrMYB24 regulates lignin and cellulose biosynthesis by binding different *cis*-elements of gene. However, AC element was not identified in the promoter of *PbrLAC4*, and PbrMYB24 could not recognize MBS element of *PbrLAC4*. We speculate that PbrMYB24 may bind to other *cis*-elements to activate the transcription of *PbrLAC4* or that it interacts with other proteins to form higher order protein–protein complexes that recognize the *PbrLAC4* promoter. *Betula platyphylla*, BplMYB4, which is a homologous protein of *PbrMYB24*, not only binds to 5 AC-box elements, MYBCORE, TC-box, GT-box, and E-box motifs involved in SCW biosynthesis and abiotic stress responses but also interacts with 5 MYBs to form heterodimers that enhance the binding to the MYBCORE motif and activate the transcription of target genes (Guo et al. 2017, 2018; Wang et al. 2019). However, we did not identify these elements in the promoters of *PbrLAC4*. In future analysis, PbrMYB24 could also be used as a bait gene to retrieve interacting TFs and then construct a more comprehensive regulatory network in the future.

The transcriptional regulatory mechanism of PbrMYB24 showed a species-specific regulatory mechanism for SCW biosynthesis in pear stone cells

SCW formation in plants is a complex process that requires at least 3 layers of TFs in a transcriptional regulatory network (Zhang et al. 2018). In the model plant *A. thaliana*, NAC TFs belong to the first layer of the network; an example is AtNST3, which directly regulates the second layer of MYB TFs, such as AtMYB46 (Ko et al. 2009; McCarthy et al. 2009). AtMYB46 regulates the third layer of MYB TFs, including AtMYB85, AtMYB58, AtMYB63, and AtMYB103, which can directly regulate the expression of structural genes (Hussey et al. 2013). The SCW synthesis regulatory network mediated by NAC-MYB TFs is relatively conserved in most plant species (Zhang et al. 2018). However, in cotton fibers, *GhMYB7*, a gene homologous to *AtMYB103*, activates the promoters of *GhFSN1*, *GhMYB46_D13*, and *GhCESA4/7/8* to promote cellulose biosynthesis (Huang et al. 2016, 2021). This means that the proteins encoded by homologous genes may have conserved functions in different species but that the transcriptional regulatory network may be somewhat different.

In our study, PbrMYB24 is found to cluster with AtMYB46, which belongs to the second layer of the regulatory network. Interestingly, PbrMYB24 not only directly activates the transcription of lignin and cellulose biosynthesis genes but also directly activates the expression of the TF-encoding genes *PbrNSC* (first layer of cascade regulation) and *PbrMYB169* (third layer of cascade regulation). In addition, *PbrMYB24* can be activated by PbrMYB169 and PbrNSC, and the overexpression of *PbrMYB24* in pear callus was found to increase the relative transcription of *PbrMYB169* and *PbrNSC*. In transgenic *Arabidopsis* plants, the expression level of *AtMYB85* is drastically increased, but transcription of *AtNST3* did not seem to change significantly. This indicates that a species-specific regulatory mechanism for SCW biosynthesis is likely present in pear stone cells, which is different from findings in model plants. Based on the abovementioned results, we speculate that *PbrNSC* (first-layer TF), *PbrMYB24* (second-layer TF), and *PbrMYB169* (third-layer TF) form a positive hierarchical regulatory system in the formation of stone cells in pear.

Establishing a high-efficiency verification system for SCW biosynthesis genes in pear callus

Plant hormones are involved in almost all aspects of plant growth and development. Auxin, a fundamental plant hormone, has been shown to negatively regulate lignin biosynthesis in pummelo juice sacs (Shi et al. 2020). A previous study showed that poplar callus can be induced to differentiate tracheary elements on MS medium without auxin but containing EBR (Yamagishi et al. 2013). In our study, we confirmed that pear callus does not synthesize lignin on MS subculture medium containing 2,4-D and 6-BA, although it did synthesize lignin on MS induction medium containing EBR but lacking 2,4-D and 6-BA. This result not only shows that the plant hormone induction system is useful for observing the phenotype in pear callus but also provides a basis for exploring the function and application of plant growth regulators in the regulation of stone cell formation.

As we know, gene function verification in perennial fruit trees is time-consuming and inefficient, mainly due to difficulties encountered in developing transformation systems

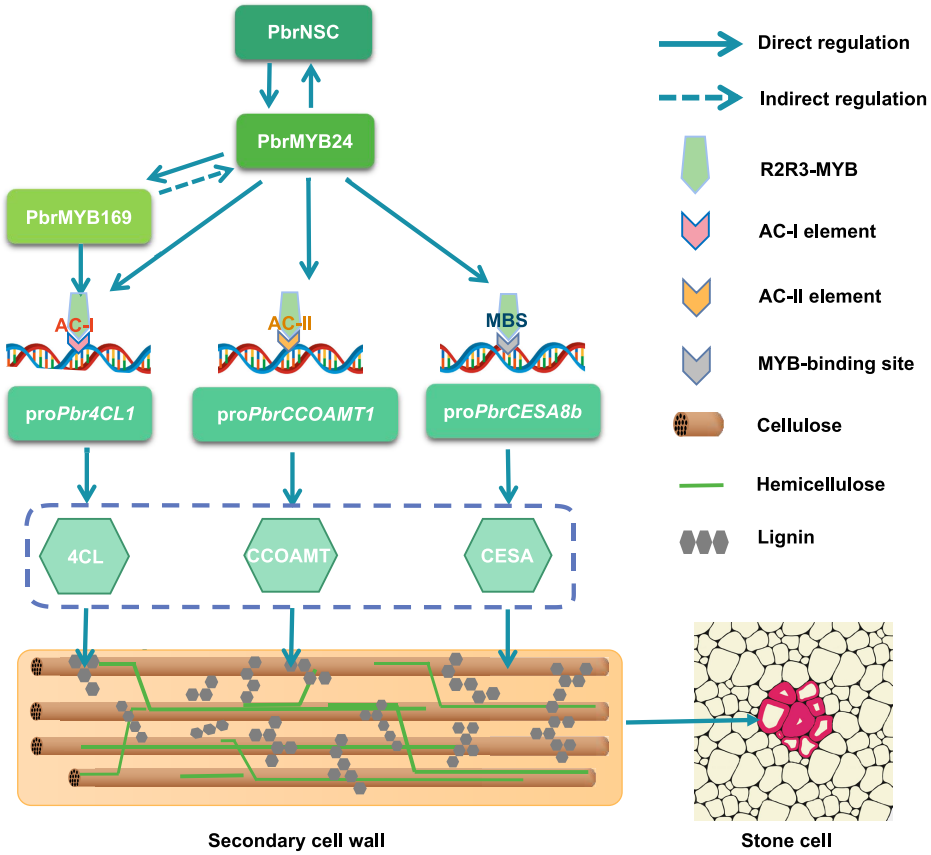

Figure 8. The hypothetical working model of PbrMYB24 regulation of stone cell formation. PbrMYB24 activates the transcription of *Pbr4CL1*, *PbrCCOAMT1*, and *PbrCESA8b* genes by binding to AC-I element, AC-II element, and MBS, respectively. In addition, PbrMYB24 binds directly to the promoters of *PbrMYB169* and *PbrNSC*, and both PbrMYB169 and PbrNSC can activate the *PbrMYB24* promoter. PbrNSC and PbrMYB169 positively regulate lignification in stone cells (Xue et al. 2019a; Wang et al. 2021).

and the very long period of time before the plants flower and produce fruits and seeds after transformation. In previous studies, instead of using model plants, apple callus and pear callus were developed and used to study the function of genes related to anthocyanin biosynthesis, which accelerates the study of gene function verification in a homologous system (Xie et al. 2012; Bai et al. 2019). Here, we developed a system to induce callus tissue in pear, which was successfully used to show that PbrMYB24 promotes lignin and cellulose biosynthesis in pear fruits. Our study provides a useful and highly efficient experimental system to accelerate the study of lignin and cellulose biosynthesis in pear fruits for the improvement of fruit quality.

Conclusion

Based on the combination of co-expression network analysis, gene expression profiles, and transcriptome analysis in a diverse group of pear accessions, we identified a MYB TF-encoding gene, *PbrMYB24*, which is significantly correlated with stone cell formation in pear fruits. Overexpression of *PbrMYB24* increased lignin and cellulose accumulation and the expression levels of SCW biosynthesis genes in pear fruits, pear callus, and *Arabidopsis* plants. Based on the further experimental results, we proposed the regulating mechanism that PbrMYB24 directly activates the transcription of lignin and cellulose biosynthesis genes by binding to AC elements and MBS (Fig. 8). Meanwhile, PbrMYB24 binds directly to the promoters of *PbrMYB169* and *PbrNSC* activating the gene expression, whereas both PbrMYB169 and PbrNSC can activate the promoter of *PbrMYB24* enhancing the gene expression (Fig. 8). Our results advance the understanding of regulatory networks that control stone cell formation and provide a gene resource for future improvement of fruit quality in pear.

Materials and methods

Plant materials

In this study, different tissues of 'Dangshansuli' pear (*P. bretschneideri*), including stems, leaves, anthers, and fruits at 21, 35, 49, 63, 77, 91, 105, and 150 DAFB, were collected from Gaoyou County, Jiangsu Province, China. The fruits of another 19 pear accessions were collected at key stages of stone cell formation from the Lishui Experiment Station, Jiangsu Academy of Agricultural Science. *Arabidopsis* (*A. thaliana*) Col-0 plants were grown in a growth chamber

at 22 °C and a 16-h light/8-h dark photoperiod. Light intensity was 10,000 lux. Pear callus was induced from the flesh of 'Clapp's Favorite' (*P. communis*) fruits and grown in the dark on solid MS medium.

RNA isolation and RT-qPCR

Total RNA was extracted from different tissues using a cetyltrimethylammonium bromide (CTAB)-based method (Porebski et al. 1997). First-strand cDNA was synthesized using the RevertAid First Strand cDNA Synthesis Kit (Transgen, China). The RT-qPCR reactions were performed using the LightCycler 480 SYBR GREEN Master system (Roche, USA). The primers used for RT-qPCR analysis are listed in Supplemental Table S1. Gene expression data were calculated using the $2^{-\Delta\Delta Ct}$ method of Livak and Schmittgen (2001). At least 3 biological replicates were included in each experiment.

Gene cloning

The coding sequence (CDS) of *PbrMYB24* was amplified from 'Dangshansuli' pear using Q5 Highly-Fidelity 2× Master Mix (New England Biolabs, Ipswich, MA, USA). The names and sequences of the primers, restriction sites, and homology arm are given in Supplemental Table S3. The *PbrMYB24* PCR products were gel-purified and cloned into the binary vector pCAMBIA1302 using the ClonExpress Entry One Step Cloning Kit (Vazyme, China). Plasmid DNA was isolated from at least 10 *Escherichia coli* colonies for DNA sequencing. The correct fusion constructs were then transformed into *A. tumefaciens* strain GV3101 using the freeze–thaw method.

Phylogenetics and analysis of *cis*-acting elements

A phylogenetic tree was constructed with the sequences of PbrMYB24 and R2R3 MYB TF proteins from other species using the neighbor-joining method as implemented in MEGA 5. The reliability of the clades was evaluated by 1,000 bootstrap resamplings. The PlantCARE database was used to identify *cis*-elements in the promoters of pear lignin biosynthesis genes.

Self-activation analysis in yeast

Self-activation analysis was performed using the Matchmaker Gold Yeast Two-Hybrid System (Clontech, http://www.clontech.com/). In order to analyze the self-activation of PbrMYB24, the entire coding region sequence and 3 N-terminal amino acid sequences ($MYB24^{1-130}$, $MYB24^{1-210}$, and $MYB24^{1-290}$) were cloned using the primers given in Supplemental Table S3 and inserted into the pGBKT7 bait vector. Following the manufacturer's instructions, the bait fusion constructs and the empty pGADT7 vector were co-transformed into yeast strain AH109 (Yeastmaker, Clontech). The AH109 cells were cultured on SD/-Trp-Leu medium for at least 48 h. The positive AH109 cells were further grown on SD/-Trp-Leu-His-Ade medium, and images were taken after 36 h.

Transient gene expression in pear fruit flesh

To transiently overexpress *PbrMYB24*, the full-length CDS of *PbrMYB24* was fused in frame to the N-terminus of GFP to form the fusion vector 35S: *PbrMYB24*-GFP. For TRV virus-induced gene silencing (VIGS), the partial CDSs of *PbrMYB24* (571 to 903 bp) were amplified using the primers given in Supplemental Table 3, and the amplified fragment was inserted into the vector TRV2. Transient gene expression in pear fruit flesh was performed according to the previously described method (Xue et al. 2019b) with some modifications. Briefly, *A. tumefaciens* GV3101 cells carrying the *PbrMYB24* overexpression or silencing constructs or the empty vector were cultured in Luria-Bertani (LB) medium to $OD_{600} = 0.9$. The cells were centrifuged and resuspended in the equal volume of infiltration buffer (10 mM MgCl2, 200 μM acetosyringone, and 10 mM MES; pH = 5.7) and then placed at 22 °C in dark for 4 h. The cells with the infiltration buffer were injected into fruit flesh tissues of 'Dangshansuli' at 35 DAFB with needle syringes. Fifteen fruits were injected per treatment, and the experiment was repeated 3 times. The injected fruits were placed in dark for 24 h and then in light with a 16-h photoperiod for 7 d at 22 °C. Sections of injected fruits were stained with phloroglucinol-HCl (Wiesner's reagent).

Genetic transformation of pear callus

Transformation of pear callus was performed according to the method given in Bai et al. (2019). Pear callus was immersed for 15 min in MS liquid medium with a suspension of GV3101 cells ($OD_{600} = 0.6$) carrying either the *PbrMYB24* overexpression vector or the empty vector control. The infected pear callus was co-cultured on solid MS medium for 48 h and then screened on solid MS subculture medium containing 20 mg/L hygromycin, 0.5 mg/L 6-BA, and 1 mg/L 2,4-D, for at least 1 mo in the dark at 24 °C. Transgenic calli were subcultured every 15 d. Subsequently, the subcultured transgenic pear calli were moved to induction medium supplemented with different concentrations of EBR but lacking 2,4-D and 6-BA (Yamagishi et al. 2013) for 20 d and were then stained with phloroglucinol-HCl (Wiesner's reagent).

Arabidopsis transformation

A. thaliana Col-0 was transformed using the floral dip method (Clough and Bent 1998) and *A. tumefaciens* GV3101 carrying the *PbrMYB24* overexpression DNA constructs. T_0 seeds were screened for transformants on MS medium containing 20 mg/L hygromycin. T_1-generation transgenic plants were analyzed using RT-qPCR with RNA extracted from inflorescence stems to determine the relative expression of *PbrMYB24*. Three lines in which *PbrMYB24* was highly expressed were selected for the subsequent experiments.

Analyses of lignin and cellulose contents

Inflorescence stems of WT and T_3 transgenic *Arabidopsis* plants and pear callus were dried to constant weights. Cell

wall residue (CWR) was extracted from 10 mg samples of the dried tissues for analysis of the lignin and cellulose contents. The extractions were performed in 2-mL centrifuge tubes for 30 min each time in phosphate buffer, methanol, chloroform, acetone, and dimethyl sulfoxide. The lignin and cellulose contents were determined using a modified acetyl bromide method and the anthrone–sulfuric acid method, respectively (Van Acker et al. 2013; Wang et al. 2021).

Histological analysis and microscopy

Two months after seed germination, the basal parts of the primary inflorescence stem of WT and *PbrMYB24*-OE transgenic *A. thaliana* plants were immersed in formalin–acetic acid–alcohol (FAA) fixative solution at 4 °C for 1 wk. The samples were treated in an ethanol concentration series [85% (*v*/*v*), 95% (*v*/*v*), and 100% (*v*/*v*)] and embedded in paraffin wax. Sections (5 μm) were cut with an automatic microtome (Leica Microsystems, Germany). In order to detect lignified cell walls, the sections were stained with toluidine blue O and safranin O–fast green and then observed using a Leica TCs SP2 spectral confocal microscope (Leica Microsystems, Germany). The lignin autofluorescence was visualized under ultraviolet light (excitation at 355/25). For cellulose visualization, the sections were stained with calcofluor white stain and examined under ultraviolet light (excitation at 355/25). The laser intensity, pinhole, and photomultiplier gain settings remain unchanged between the different samples.

For scanning electron microscopy (SEM), the stem sample was fixed in fresh 2.5% (*v*/*v*) glutaraldehyde stationary solution. A vacuum treatment was used to keep the sample completely immersed in the fixative for 12 h. Image-Pro Plus software was used to measure the thickness of SCW of interfascicular fiber and vessel cells on the images.

Dual-luciferase reporter assays in *N. benthamiana* leaves

In order to determine the effect of PbrMYB24 on the expression of *PbrMYB169*, *PbrNSC*, and SCW biosynthesis genes, their promoters and mutated promoters (*Pbr4CL1-AC-D*, *PbrCCOAMT1-AC-D*, *PbrLAC4-MBS-D*, *PbrLAC19-AC-D*, and *PbrLAC19-MBS-D*) were amplified with primers listed in Supplemental Table S1 and inserted into the pGreenII 0800-LUC vector as reporter genes, which was then introduced into *A. tumefaciens* strain GV3101 (pSoup) competent cells. The effector vector was the PbrMYB24 overexpression construct, and the empty vector was used as a control. The *Agrobacterium* cells containing the effector vector or the reporter vector were mixed with the cells containing a reporter construct in a proportion of 9:1 in an infiltration buffer (10 mM $MgCl_2$, 200 μM acetosyringone, and 10 mM MES) to a final concentration of $OD_{600} = 0.9$ to 1.0. The mixed cells were infiltrated into leaves of 2-wk-old *N. benthamiana* plants. The activities of LUC and REN were detected 48 h later with a dual LUC assay kit (Promega, USA) using a microplate reader (Molecular Devices, USA). The transcriptional activation ability of PbrMYB24 was evaluated by LUC/REN ratio.

Y1H assay analysis

The CDS of PbrMYB24 and the *Pbr4CL1* and *PbrCCOMT2* promoter fragments containing the AC elements were cloned and inserted into the pGADT7 vector and the pABAi vector, respectively. The bait plasmid was then linearized and integrated into Y1H Gold Yeast (Clontech, http://www.clontech.com). The transformants were then screened on SD/-Ura medium supplemented with 0, 100×, 200×, and 300× ABA. The interactions between PbrMYB24 and the promoters were detected on SD/-Leu medium with the optimum AbA concentration. The empty pGADT7 vector of the corresponding recombinant pABAi was used as the negative control, and p53-AbAi was used as positive control. Images of the colonies were taken after 48 h of culture.

The PbrMYB24 CDS was fused with the activation domain (B42AD) to construct the effector (pB42AD-MYB24). The promoters of the SCW biosynthesis genes and the mutated promoters (*Pbr4CL1-AC-D*, *PbrCCOAMT1-AC-D*, and *PbrCESA8b-MBS-D*) were cloned and inserted into pLacZi vector to construct the reporters. The reporters and effector were co-transformed into the yeast strain EGY48 as described in the Yeast Protocols Handbook (Clontech). The co-transformed yeast cells were cultured on SD/-Trp-Ura medium containing X-gal to observe the color development of the yeast colonies. The empty pB42AD vector of the corresponding recombinant pLaczi was used as the negative control. Images were taken after 48 to 72 h.

Electrophoretic mobility shift assay

The CDS of PbrMYB24 was cloned and inserted into the Pcold TF prey vector. The fusion constructs were transferred into *E. coli* strain BL21 for protein expression. The probe containing the AC elements in the promoter of *PbrCCOAMT1* was synthesized and biotin-labeled at the 3′ end by Sangon Biotech Company (China). The biotin-labeled DNA fragments were incubated for 30 min with MYB24-MBP in binding buffer [50 mM KCl, 5 mM $MgCl_2$, 0.05% Nonidet P-40, 2.5% glycerol, 1 mM DTT, and 10 mM Tris (pH 7.5)]. For competition analysis, unlabeled probe was included in the binding reactions at 10× and 50× molar excess relative to the labeled probes. The DNA fragments bound to MYB24-MBP were separated from the unbound probe by 6% nondenaturing polyacrylamide gel electrophoresis (PAGE), and the DNA probe and DNA–protein complexes were transferred to a nitrocellulose membrane and detected using a Chemiluminescent Detection Kit (Beyotime, China).

Firefly LCI

Firefly LCI with pCAMBIA-nLUC and pCAMBIA-cLUC vectors was used to verify the protein–protein interactions. The *PbrMYB24* CDS was cloned into the pCAMBIA-nLUC vector, and *PbrMYB169* was cloned into the pCAMBIA-cLUC vector. Equal amounts of *A. tumefaciens* cultures

carrying the PbrMYB24-cLUC and PbrMYB169-nLUC constructs were co-infiltrated into the leaves of *N. benthamiana* plants. Luciferase activity was observed 2 d after infiltration by spraying 1 mM luciferin on the leaves. LUC images were captured using a deep cooled CCD imaging apparatus (Tanon 5200 multichemiluminescent imaging system).

Statistical analysis

The data were statistically processed using SPSS software (IBM, USA); Student's *t* test was used to compare the statistical significance of 2 populations at $^{*}P < 0.05$. One-way ANOVA and Tukey's test were used to compare the significance among 3 or more populations. The different letters above the error bar indicate significance. Pearson's correlations were obtained using the *cor*.test.

Accession numbers

Sequence data from this article can be found in the GenBank/EMBL data libraries under accession numbers PbrMYB169 (*MG594365*), PbrNSC (*MK720951*), p*Pbr4CL1* (*MG594366*), p*Pbr4CL4* (*MG594367*), p*PbrC3′H1* (*MG594368*), p*PbrHCT33* (*MG594371*), pPbr*CCOAMT1* (*MG594372*), p*PbrCAD24* (*MG594373*), p*PbrCCR21* (*MG594374*), p*PbrCCR23* (*MG594375*), p*PbrLAC4* (*MG594378*), p*PbrLAC5* (*MG594377*), pPbr*LAC19* (*MG594380*), p*PbrMYB169* (*MK720952*), and p*PbrNSC* (*MK720953*). The sequence data of Pbr017813.1 (*PbrMYB24*) can be found in the pear genome database (http://peargenome.njau.edu.cn).

Acknowledgments

We thank the state Key Laboratory of Crop Genetics and Germplasm Enhancement and Utilization, the Centre of Pear Engineering Technology Research, Nanjing Agricultural University for supporting this project.

Author contributions

J.W. and Y.X. conceived and designed the experiments. Y.S. and Y.X. performed the experiments. C.X., R.W., and S.X. performed the data analysis. J.Y. provided suggestions for experiments and revised the manuscript. D.L. and Z.Y. collected the phenotype data. J.L. and X.L. provided pear fruit materials. Y.X., C.X., and J.W. wrote and revised the manuscript.

Supplemental data

The following materials are available in the online version of this article.

Supplemental Figure S1. RNA-seq data show the expression profiles of *PbrMYB88* and *PbrMYB24* during fruit development DAFB in 5 pear cultivars.

Supplemental Figure S2. RT-qPCR was used to determine the expression levels of PbrMYB24 in different tissues and fruits at 8 developmental stages DAFB of 'Dangshansuli' pear plants.

Supplemental Figure S3. RT-qPCR assays were used to determine the relative expression of *PbrMYB24* in pear flesh tissue around the infiltration sites.

Supplemental Figure S4. An induction system for lignin biosynthesis in pear callus.

Supplemental Figure S5. Phenotypic observation of transgenic *A. thaliana* Col-0 plants overexpressing *PbrMYB24*.

Supplemental Figure S6. Schematic diagrams showing the effector and reporter gene constructs used in the dual-luciferase assays.

Supplemental Figure S7. Analysis of self-activation in the *Pbr4CL1* and *PbrCCOMT2* promoters.

Supplemental Figure S8. SDS-PAGE analysis of the PbrMYB24 protein expressed in *E. coli* following induction by IPTG.

Supplemental Figure S9. Firefly luciferase complementation assay showing that PbrMYB24 does not interact with PbrMYB169 in *N. benthamiana* leaf cells.

Supplemental Figure S10. Firefly luciferase complementation assay showing that PbrMYB24 does not interact with PbrNSC in *N. benthamiana* leaf cells.

Supplemental Table S1. Known plant R2R3 MYBs used in the phylogenetic analysis in this study.

Supplemental Table S2. The AC/MBS sequence information in different SCW biosynthesis genes.

Supplemental Table S3. The information of the homology arm, primer, and restriction site used in this study.

Funding

This work was funded by the National Science Foundation of China (32230097 and 32172531), the Earmarked Fund for China Agriculture Research System (CARS-28), the Earmarked Fund for Jiangsu Agricultural Industry Technology System JATS [2022]454, and the Natural Science Foundation of Jiangsu Province for Young Scholar (BK20221010).

Conflict of interest statement. None declared.

References

Bai SL, Tao RY, Tang YX, Yin L, Ma YJ, Ni JB, Yan XH, Yang QS, Wu ZY, Zeng Y, et al. BBX16, a B-box protein, positively regulates light-induced anthocyanin accumulation by activating MYB10 in red pear. Plant Biotechnol J. 2019:**17**(10):1985–1997. https://doi.org/10.1111/pbi.13114

Bao L, Chen KS, Zhang D, Cao YF, Yamamoto T, Teng YW. Genetic diversity and similarity of pear (*Pyrus* L.) cultivars native to east Asia revealed by SSR (simple sequence repeat) markers. Genet Resour Crop Evol. 2007:**54**(5):959–971. https://doi.org/10.1007/s10722-006-9152-y

Bhargava A, Mansfield SD, Hall HC, Douglas CJ, Ellis BE. MYB75 functions in regulation of secondary cell wall formation in the *Arabidopsis* inflorescence stem. Plant Physiol. 2010:**154**(3):1428–1438. https://doi.org/10.1104/pp.110.162735

Cao YP, Han YH, Li DH, Lin Y, Cai YP. MYB transcription factors in Chinese pear (*Pyrus bretschneideri* Rehd.): genome-wide identification, classification, and expression profiling during fruit

development. Front Plant Sci. 2016:**7**(4): 577. https://doi.org/10.3389/fpls.2016.00577

Cao YP, Meng DD, Li XX, Wang LH, Cai YP, Jiang L. A Chinese white pear (*Pyrus bretschneideri*) BZR gene *PbBZR1* act as a transcriptional repressor of lignin biosynthetic genes in fruits. Front Plant Sci. 2020:**11**(7):1087. https://doi.org/10.3389/fpls.2020.01087

Cheng X, Li GH, Muhammad A, Zhang JY, Jiang TS, Jin Q, Zhao H, Cai YP, Lin Y. Molecular identification, phylogenomic characterization and expression patterns analysis of the LIM (LIN-11, isl1 and MEC-3 domains) gene family in pear (*Pyrus bretschneideri*) reveal its potential role in lignin metabolism. Gene 2019:**686**(2):237–249. https://doi.org/10.1016/j.gene.2018.11.064

Clough SJ, Bent AF. Floral dip: a simplified method for *Agrobacterium*-mediated transformation of *Arabidopsis thaliana*. Plant J. 1998:**16**(6): 735–743. https://doi.org/10.1046/j.1365-313x.1998.00343.x

Geng P, Zhang S, Liu JY, Zhao CH, Wu J, Cao YP, Fu CX, Han X, He H, Zhao Q. MYB20, MYB42, MYB43, and MYB85 regulate phenylalanine and lignin biosynthesis during secondary cell wall formation. Plant Physiol. 2020:**182**(3):1272–1283. https://doi.org/10.1104/pp.19.01070

Guo HY, Wang YC, Wang LQ, Hu P, Wang YM, Jia YY, Zhang CR, Zhang Y, Zhang YM, Wang C, et al. Expression of the MYB transcription factor gene *BplMYB46* affects abiotic stress tolerance and secondary cell wall deposition in *Betula platyphylla*. Plant Biotechnol J. 2017:**15**(1):107–121. https://doi.org/10.1111/pbi.12595

Guo HY, Wang LQ, Yang CP, Zhang YM, Zhang CR, Wang C. Identification of novel *cis*-elements bound by BplMYB46 involved in abiotic stress responses and secondary wall deposition. J Integr Plant Biol. 2018:**60**(10):1000–1014. https://doi.org/10.1111/jipb.12671

Huang JF, Chen F, Guo YJ, Gan XL, Yang MM, Zeng W, Persson S, Li J, Xu WL. GhMYB7 promotes secondary wall cellulose deposition in cotton fibres by regulating *GhCesA* gene expression through three distinct *cis*-elements. New Phytol. 2021:**232**(4):1718–1737. https://doi.org/10.1111/nph.17612

Huang JF, Chen F, Wu SY, Li J, Xu WL. Cotton *GhMYB7* is predominantly expressed in developing fibers and regulates secondary cell wall biosynthesis in transgenic *Arabidopsis*. Sci China Life Sci. 2016:**59**(2): 194–205. https://doi.org/10.1007/s11427-015-4991-4

Hussey SG, Mizrachi E, Creux NM, Myburg AA. Navigating the transcriptional roadmap regulating plant secondary cell wall deposition. Front Plant Sci. 2013:**4**(8):325. https://doi.org/10.3389/fpls.2013.00325

Ithal N, Reddy AR. Rice flavonoid pathway genes, OsDfr and OsAns, are induced by dehydration, high salt and ABA, and contain stress responsive promoter elements that interact with the transcription activator, OsC1-MYB. Plant Sci. 2004:**166**(6):1505–1513. https://doi.org/10.1016/j.plantsci.2004.02.002

Jin H, Cominelli E, Bailey P, Parr A, Mehrtens F, Jones J, Tonelli C, Weisshaar B, Martin C. Transcriptional repression by AtMYB4 controls production of UV-protecting sunscreens in *Arabidopsis*. Embo J. 2000:**19**(22):6150–6161. https://doi.org/10.1093/emboj/19.22.6150

Kim WC, Ko JH, Han KH. Identification of a *cis*-acting regulatory motif recognized by MYB46, a master transcriptional regulator of secondary wall biosynthesis. Plant Mol Biol. 2012:**78**(4-5):489–501. https://doi.org/10.1007/s11103-012-9880-7

Ko JH, Jeon HW, Kim WC, Kim JY, Han KH. The MYB46/MYB83-mediated transcriptional regulatory programme is a gatekeeper of secondary wall biosynthesis. Ann Bot. 2014:**114**(6):1099–1107. https://doi.org/10.1093/aob/mcu126

Ko JH, Kim WC, Han KH. Ectopic expression of *MYB46* identifies transcriptional regulatory genes involved in secondary wall biosynthesis in *Arabidopsis*. Plant J. 2009:**60**(4):649–665. https://doi.org/10.1111/j.1365-313X.2009.03989.x

Li XL, Xue C, Li JM, Qiao X, Li LT, Yu L, Huang YH, Wu J. Genome-wide identification, evolution and functional divergence of MYB transcription factors in Chinese white pear (*Pyrus bretschneideri*). Plant Cell Physiol. 2016:**57**(4):824–847. https://doi.org/10.1093/pcp/pcw029

Liu JY, Osbourn A, Ma PD. MYB transcription factors as regulators of phenylpropanoid metabolism in plants. Mol Plant 2015:**8**(5): 689–708. https://doi.org/10.1016/j.molp.2015.03.012

Livak KJ, Schmittgen TD. Analysis of relative gene expression data using real-time quantitative PCR and the 2(-Delta Delta C(T)) method. Methods 2001:**25**(4):402–408. https://doi.org/10.1006/meth.2001.1262

Martín-Cabrejas MA, Aguilera Y, Benítez V, Mollá E, López-Andréu FJ, Esteban RM. Effect of industrial dehydration on the soluble carbohydrates and dietary fiber fractions in legumes. J Agric Food Chem. 2006:**54**(20):7652–7657. https://doi.org/10.1021/jf061513d

Mccarthy RL, Zhong R, Ye ZH. *MYB83* is a direct target of SND1 and acts redundantly with MYB46 in the regulation of secondary cell wall biosynthesis in *Arabidopsis*. Plant Cell Physiol. 2009:**50**(11): 1950–1964. https://doi.org/10.1093/pcp/pcp139

Öhman D, Demedts B, Kumar M, Gerber L, Gorzsás A, Goeminne G, Hedenström M, Ellis B, Boerjan W, Sundberg B. MYB103 is required for FERULATE-5-HYDROXYLASE expression and syringyl lignin biosynthesis in *Arabidopsis* stems. Plant J. 2013:**73**(1):63–76. https://doi.org/10.1111/tpj.12018

Porebski S, Bailey LG, Baum BR. Modification of a CTAB DNA extraction protocol for plants containing high polysaccharide and polyphenol components. Plant Mol Biol Rep. 1997:**15**(1):8–15. https://doi.org/10.1007/BF02772108

Preston J, Wheeler J, Heazlewood J, Li SF, Parish RW. AtMYB32 is required for normal pollen development in *Arabidopsis thaliana*. Plant J. 2004:**40**(6):979–995. https://doi.org/10.1111/j.1365-313X.2004.02280.x

Rahantamalala A, Rech P, Martinez Y, Chaubet-Gigot N, Grima-Pettenati J, Pacquit V. Coordinated transcriptional regulation of two key genes in the lignin branch pathway CAD and CCR is mediated through MYB-binding sites. BMC Plant Biol. 2010:**10**(1): 130. https://doi.org/10.1186/1471-2229-10-130

Rogers LA, Campbell MM. The genetic control of lignin deposition during plant growth and development. New Phytologist. 2004:**164**(1):17–30. https://doi.org/10.1111/j.1469-8137.2004.01143.x

Seo MS, Kim JS. Understanding of MYB transcription factors involved in glucosinolate biosynthesis in *Brassicaceae*. Molecules 2017:**22**(9): 1549. https://doi.org/10.3390/molecules22091549

Shannon P, Markiel A, Ozier O, Baliga NS, Wang JT, Ramage D, Amin N, Schwikowski B, Ideker T. Cytoscape: a software environment for integrated models of biomolecular interaction networks. Genome Res. 2003:**13**(11):2498–2504. https://doi.org/10.1101/gr.1239303

Shi MY, Liu X, Zhang HP, He ZY, Yang HB, Chen JJ, Feng J, Yang WH, Jiang YW, Yao JL, et al. The IAA- and ABA-responsive transcription factor CgMYB58 upregulates lignin biosynthesis and triggers juice sac granulation in pummelo. Hortic Res. 2020:**7**(1):139. https://doi.org/10.1038/s41438-020-00360-7

Smita S, Katiyar A, Chinnusamy V, Pandey DM, Bansal KC. Transcriptional regulatory network analysis of MYB transcription factor family genes in rice. Front Plant Sci. 2015:**6**(12): 1157. https://doi.org/10.3389/fpls.2015.01157

Soler M, Camargo ELO, Carocha V, Cassan-Wang H, San Clemente H, Savelli B, Hefer CA, Paiva JAP, Myburg AA, Grima-Pettenati J. The *Eucalyptus grandis* R 2 R 3-MYB transcription factor family: evidence for woody growth-related evolution and function. New Phytologist 2015:**206**(4):1364–1377. https://doi.org/10.1111/nph.13039

Taylor-Teeples M, Lin L, De Lucas M, Turco G, Toal TW, Gaudinier A, Young NF, Trabucco GM, Veling MT, Lamothe R. An *Arabidopsis* gene regulatory network for secondary cell wall synthesis. Nature 2015:**517**(7536):571–575. https://doi.org/10.1038/nature14099

Van Acker R, Vanholme R, Storme V, Mortimer JC, Dupree P, Boerjan W. Lignin biosynthesis perturbations affect secondary cell wall composition and saccharification yield in *Arabidopsis thaliana*. Biotechnol Biofuels 2013:**6**(1):46. https://doi.org/10.1186/1754-6834-6-46

Van Schie CCN, Haring MA, Schuurink RC. Regulation of terpenoid and benzenoid production in flowers. Curr Opin Plant Biol. 2006:**9**(2):203–208. https://doi.org/10.1016/j.pbi.2006.01.001

Wang YM, Wang C, Guo HY, Wang YC. BplMYB46 from *Betula platyphylla* can form homodimers and heterodimers and is involved in salt and osmotic stresses. Int J Mol Sci. 2019:**20**(5):1171. https://doi.org/10.3390/ijms20051171

Wang RZ, Xue YS, Fan J, Yao JL, Qin MF, Lin T, Lian Q, Zhang MY, Li XL, Li JM, et al. A systems genetics approach reveals PbrNSC as a regulator of lignin and cellulose biosynthesis in stone cells of pear fruit. Genome Biol. 2021:**22**(1):313. https://doi.org/10.1186/s13059-021-02531-8

Wu J, Wang ZW, Shi ZB, Zhang S, Ming R, Zhu SL, Khan MA, Tao ST, Korban SS, Wang H, et al. The genome of the pear (*Pyrus bretschneideri* Rehd.). Genome Res. 2013:**23**(2):396–408. https://doi.org/10.1101/gr.144311.112

Xie XB, Li S, Zhang RF, Zhao J, Chen YC, Zhao Q, Yao YX, You CX, Zhang XS, Hao YJ. The bHLH transcription factor MdbHLH3 promotes anthocyanin accumulation and fruit colouration in response to low temperature in apples. Plant Cell Environ. 2012:**35**(11):1884–1897. https://doi.org/10.1111/j.1365-3040.2012.02523.x

Xu WJ, Dubos C, Lepiniec L. Transcriptional control of flavonoid biosynthesis by MYB–bHLH–WDR complexes. Trends Plant Sci. 2015:**20**(3):176–185. https://doi.org/10.1016/j.tplants.2014.12.001

Xue C, Yao JL, Qin MF, Zhang MY, Allan AC, Wang DF, Wu J. Pbrmir397a regulates lignification during stone cell development in pear fruit. Plant Biotechnol J. 2019b:**17**(1):103–117. https://doi.org/10.1111/pbi.12950

Xue C, Yao JL, Xue YS, Su GQ, Wang L, Lin LK, Allan AC, Zhang SL, Wu J. PbrMYB169 positively regulates lignification of stone cells in pear fruit. J Exp Bot. 2019a:**70**(6):1801–1814. https://doi.org/10.1093/jxb/erz039

Yamagishi Y, Yoshimoto J, Uchiyama H, Nabeshima E, Nakaba S, Watanabe U, Funada R. In vitro induction of secondary xylem-like tracheary elements in calli of hybrid poplar (*Populus sieboldii* × *P. grandidentata*). Planta 2013:**237**(4):1179–1185. https://doi.org/10.1007/s00425-013-1839-7

Zhang JY, Jm L, Xue C, Wang RZ, Wu J. The variation of stone cell content in 236 germplasms of sand pear (*Pyrus pyrifolia*) and identification of related candidate genes. Hortic Plant J. 2020:**7**(2):108–116. https://doi.org/10.1016/j.hpj.2020.09.003

Zhang J, Xie M, Tuskan GA, Muchero W, Chen JG. Recent advances in the transcriptional regulation of secondary cell wall biosynthesis in the woody plants. Front Plant Sci. 2018:**9**(10): 1535. https://doi.org/10.3389/fpls.2018.01535

Zhang MY, Xue C, Hu H, Li J, Xue Y, Wang R, Fan J, Zou C, Tao S, Qin M, et al. Genome-wide association studies provide insights into the genetic determination of fruit traits of pear. Nat Commun. 2021:**12**(1):1144. https://doi.org/10.1038/s41467-021-21378-y

Zhao SG, Zhang JG, Zhao YP, Zhang YX. New discoveries of stone cell differentiation in fruitlets of 'yali' pears (*Pyrus bretschneideri* Rehd.). Int J Food Agric Environ. 2013:**11**(3): 937–94. https://www.researchgate.net/publication/286229695.

Zhong RQ, Cui DT, Ye ZH. Secondary cell wall biosynthesis. New Phytol. 2019:**221**(4):1703–1723. https://doi.org/10.1111/nph.15537

Zhong RQ, Lee CH, Zhou JL, Mccarthy RL, Ye ZH. A battery of transcription factors involved in the regulation of secondary cell wall biosynthesis in *Arabidopsis*. Plant Cell 2008:**20**(10):2763–2782. https://doi.org/10.1105/tpc.108.061325

Zhong RQ, Richardson EA, Ye ZH. The MYB46 transcription factor is a direct target of SND1 and regulates secondary wall biosynthesis in Arabidopsis. Plant Cell 2007:**19**(9):2776–2792. https://doi.org/10.1105/tpc.107.053678

Zhong RQ, Ye ZH. MYB46 and MYB83 bind to the SMRE sites and directly activate a suite of transcription factors and secondary wall biosynthetic genes. Plant Cell Physiol. 2012:**53**(2):368–380. https://doi.org/10.1093/pcp/pcr185

Zhou J, Lee C, Zhong R, Ye ZH. MYB58 and MYB63 are transcriptional activators of the lignin biosynthetic pathway during secondary cell wall formation in *Arabidopsis*. Plant Cell 2009:**21**(1):248–266. https://doi.org/10.1105/tpc.108.063321